Role of microstructure in modeling of manufacturing Processes

Asim Tewari
National Center for Aerospace Innovation and Research
Department of Mechanical Engineering
Indian Institute of Technology, Bombay

TEQIP, IIT Bombay Dec 22-23, 2014

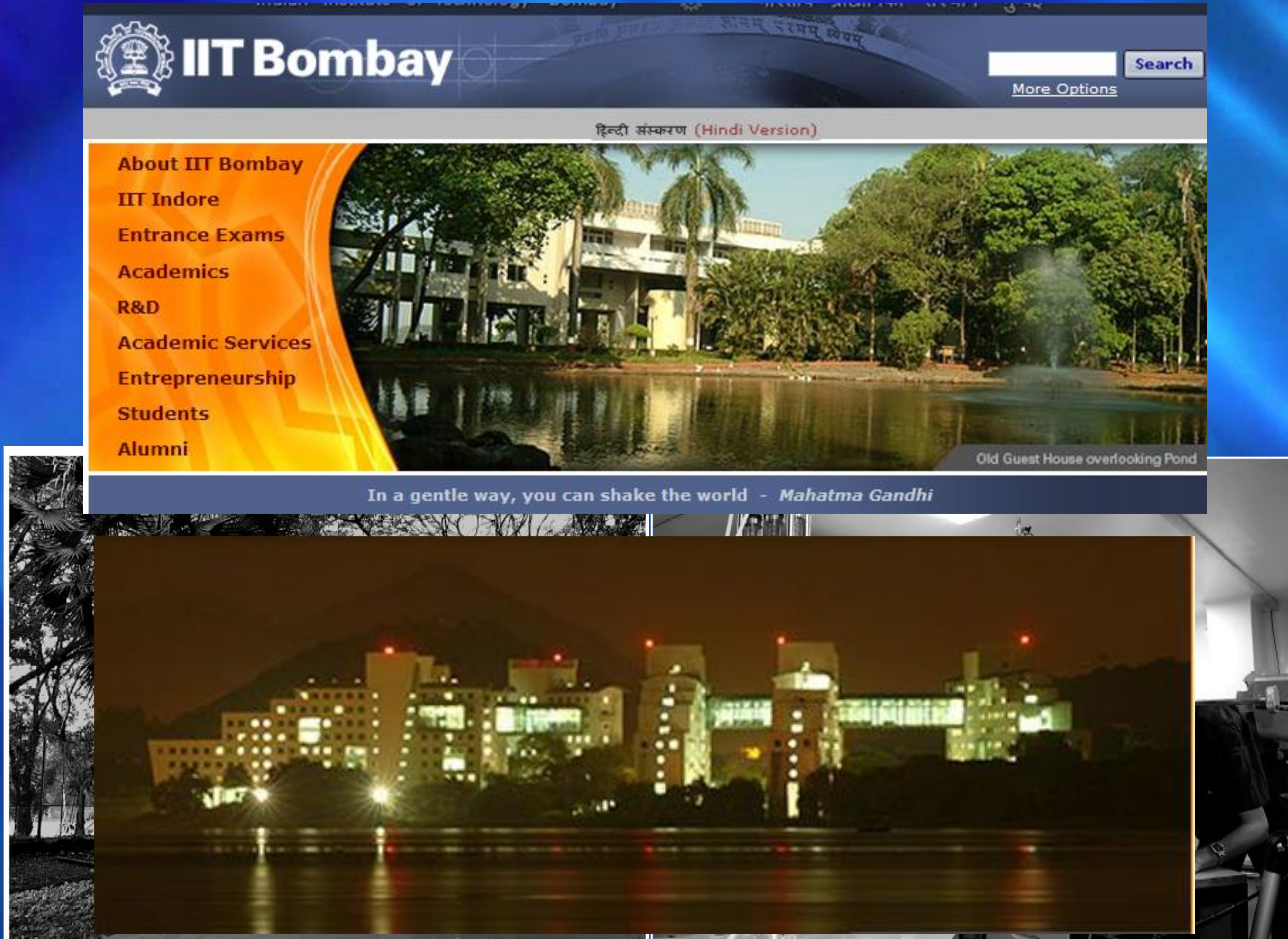
IIT Bombay
Search
More Options
हिन्दी संस्करण (Hindi Version)
About IIT Bombay
IIT Indore
Entrance Exams
Academics
R&D
Academic Services
Entrepreneurship
Students
Alumni
Old Guest House overlooking Pond
In a gentle way, you can shake the world - Mahatma Gandhi

IIT BOMBAY AT A GLANCE

Engages in research, education, training, technology development and related activities in most areas of technology, science & management

- 530 acres (5.3 sq. km) of campus area
- 15 Departments, 1 School, 4 IDPs & 9 Centers
- ~600 fulltime faculty & 90 adjunct faculty
- ~1300 support staff
- ~9600 students (P.G ~ 6000; PhD~2000)
- ~750 project research staff

Patents (India and Foreign) 2012-2013	>100
Number of industries which come to us for projects	>2000
Research funding in INR (Governmental & Industrial, 2012-13)	~300 Cr
Number of technology spinoffs from IITB technologies	>50

Overview of NCAIR

Vision

- Create a World Class Aerospace Ecosystem in India

Mission

- To be a catalyst for collaboration between industry, Academia, R&D Organizations and Government
- To provide economically viable and sustainable solutions
- To promote Innovation, Knowledge Creation and Entrepreneurship
- To disseminate knowhow and develop human resources

Inception

19th November 2010

Stake-holders

NCAIR: DST, IIT-B, Sandvik, Delcam, BOEING, DMG-Mori Seiki, NAL, HAL

Key Strategic Technologies

- Machining
- Forming
- Casting

Scope of Materials

- Titanium
- Super Alloys
- Composites
- Aluminum, Magnesium, AHSS

Services of NCAIR

Core Services

- ✓R&D Projects
- ✓Technology Transfer

Enabling Services

- ✓ Specialized Training Programs
- ✓ Adv Aero Mfg and testing facilities for R&T Activities
- ✓ Mentoring and business Services

CORE FACULTY -IITB (NCAIR)

Faculty members	Previous affiliations	Faculty members	Previous affiliations
Prof. Suhas Joshi 	IIT-Bombay, UIUC	Prof. B. Ravi 	IISc Bangalore, Purdue U
Prof. Asim Tewari 	Georgia Tech, GM Global R&D	Prof. Ramesh Singh 	Georgia Tech
Prof. S.S.Pande 	IIT-Bombay, U. Of Cincinnati	Prof. Sushil Mishra 	IIT-Bombay, GM Global R&D
Prof. Prita Pant 	Cornell University	Prof. V. Kartik 	Carnegie Mellon U, IBM Research
Prof. Shiva G. 	University of Massachusetts Amherst	Prof. Parag Tandaiya 	IISc Bangalore, Caltech, USA
Prof. Rajneesh Bharadwaj 	Johns Hopkins University, Baltimore	Prof. Rakesh G Mote 	Nanyang Technological University, Singapore.

What is microstructure?

A microstructure is an arrangement of volumes, internal surfaces, lines, and points

Volumes: Voids, fibers, inclusions, particles, grains, etc.

Surfaces: Micro-crack surfaces, grain boundaries, inclusion interfaces, etc

Lines: Dislocation lines, micro-crack tips, grain edges, triple lines, etc.

Points: Quadruple points, particle/grain centers, atoms, etc.

Texture is a part of structure and thus microstructure

Most general definition

Microstructure is a spatially (and/or temporally) varying *d* dimensional data structure.

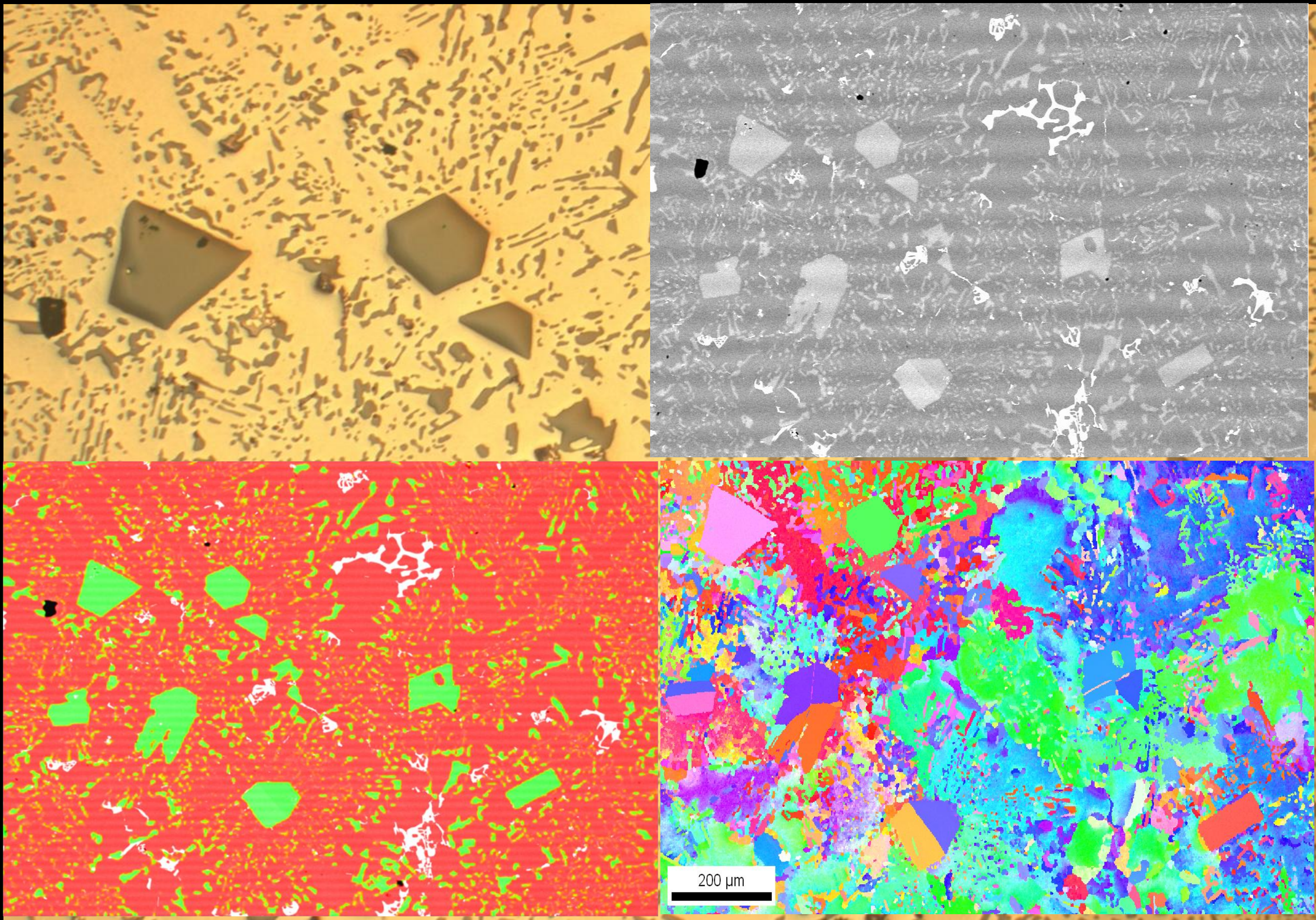
200 µm

Modalities of acquisition

- Optical
- SEM
- TEM
- AFM
- SPM
- X-ray CT
- PET, MRI, SIMS, etc.

Larger to smaller

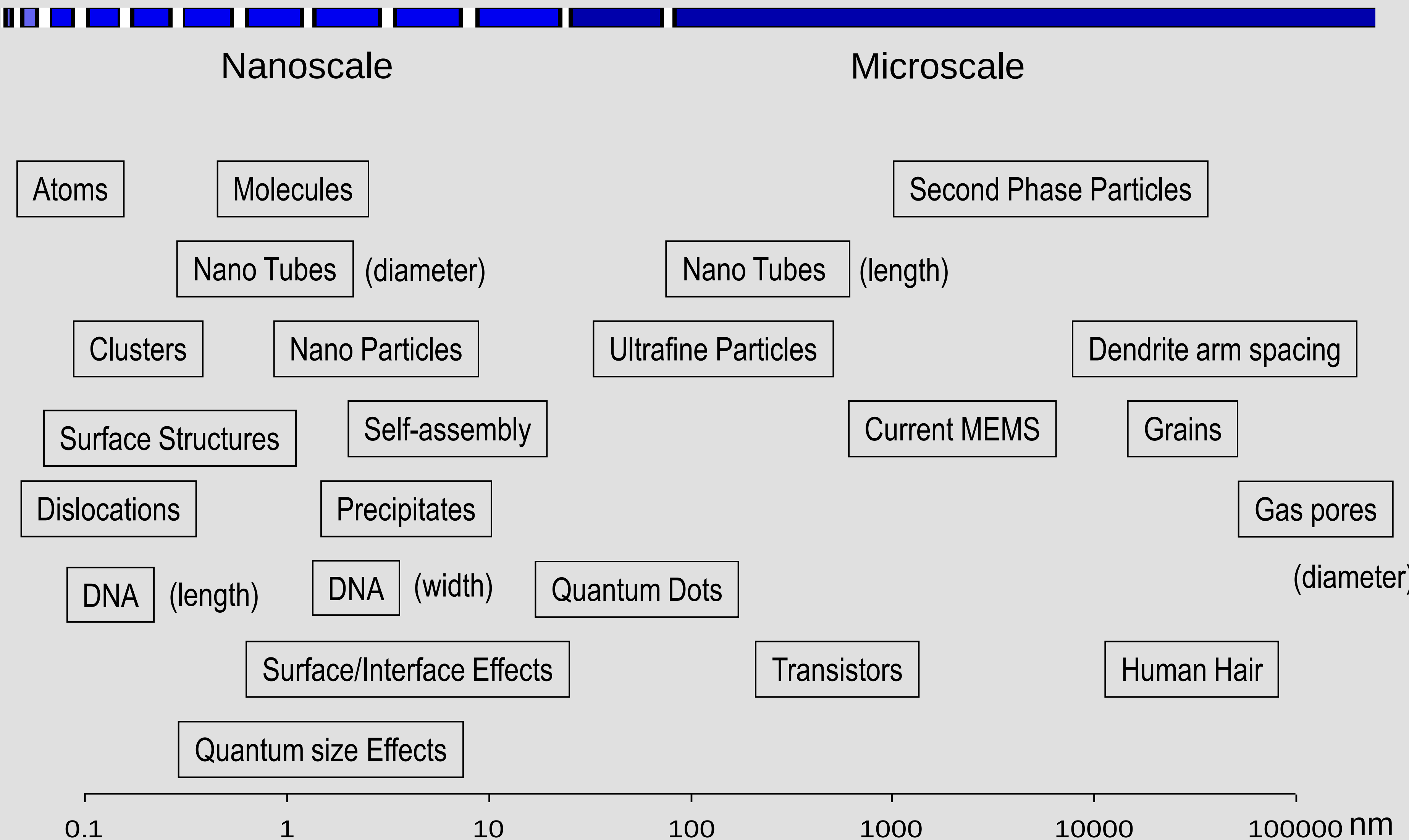

Problem of spheres in 3D

3D

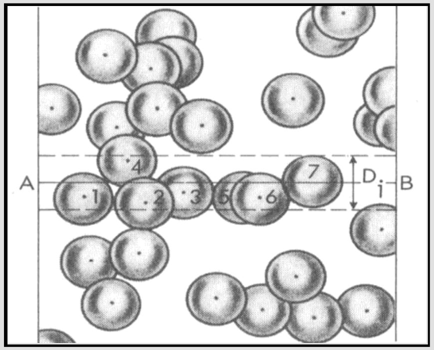

2D

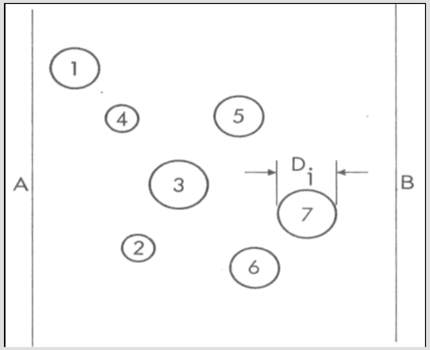

For a collection of spheres of different sizes in 3D which of the following is true:

1.) Mean circle size in 2D is <u>less than</u> mean 3D sphere size

2.) Mean circle size in 2D is <u>greater than</u> mean 3D sphere size

3.) Mean circle size in 2D is <u>equal to</u> mean 3D sphere size

Non-trivial problem

On a unit line segment choose two random points x_1 and x_2. If the points are *d* distance apart (without regard to ordering), what value of *d* has the highest probability?

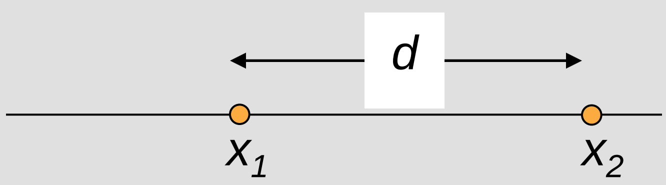

$$P(d) = \frac{\int_0^1 \int_0^1 \delta(d - |x_2 - x_1|)\, dx_1\, dx_2}{\int_0^1 \int_0^1 dx_1\, dx_2} = 2(1 - d),$$

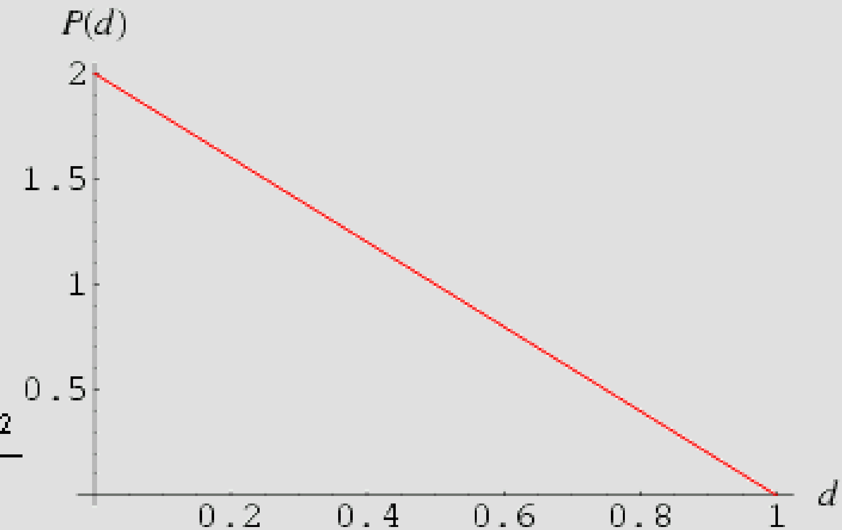

Stereology : True three-dimensional probe

- Pioneering work on
- 3D spatial statistics
- topological connectivity
- Euler-Poincare

- Approach
- through 3D reconstruction
- grains modeled as ext. convex rings

- Materials System
- A356 alloy
- AA5754 alloy
- AZ31 alloy
- THA

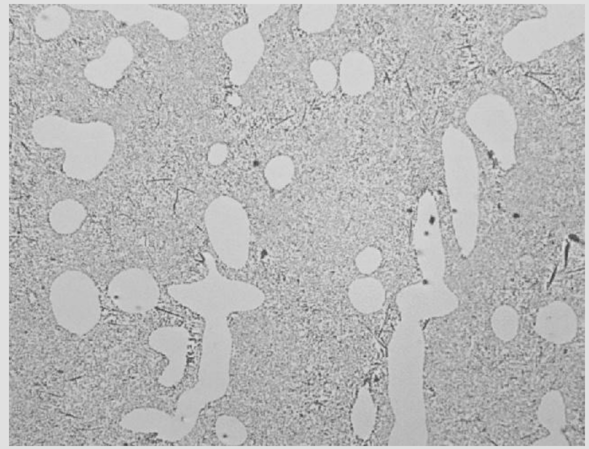

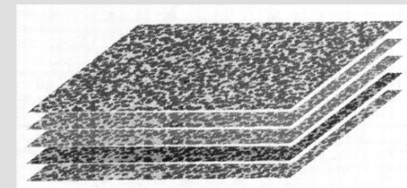

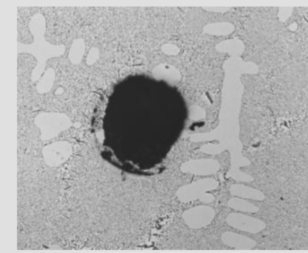

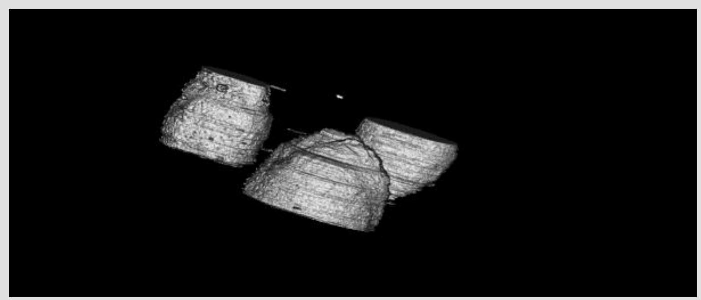

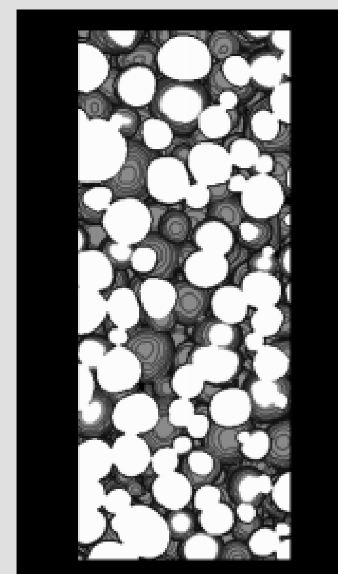

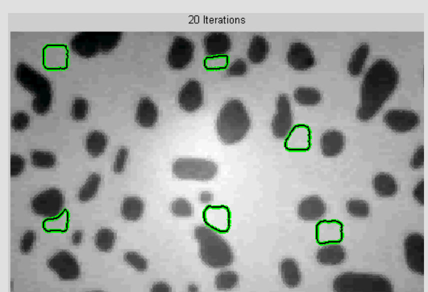

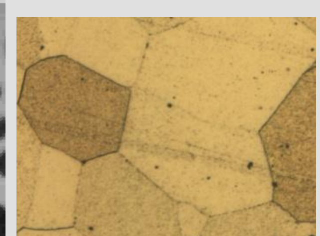

Case Study 1

Titanium alloy machining

Motivation

Gas turbine engine, compressor parts, airframe structure, Landing gear disc

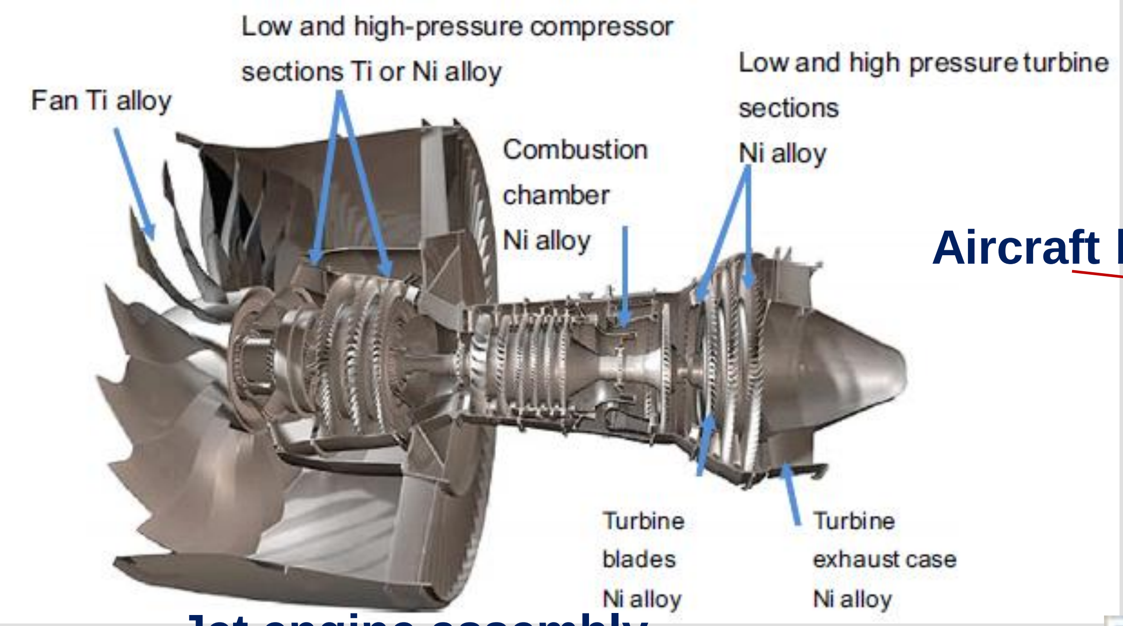

Jet engine assembly

Aircraft bolts

Bladed impeller disk

Airframe

Percentage of Airframe Titanium vs. Year of Rollout—Commercial Transports

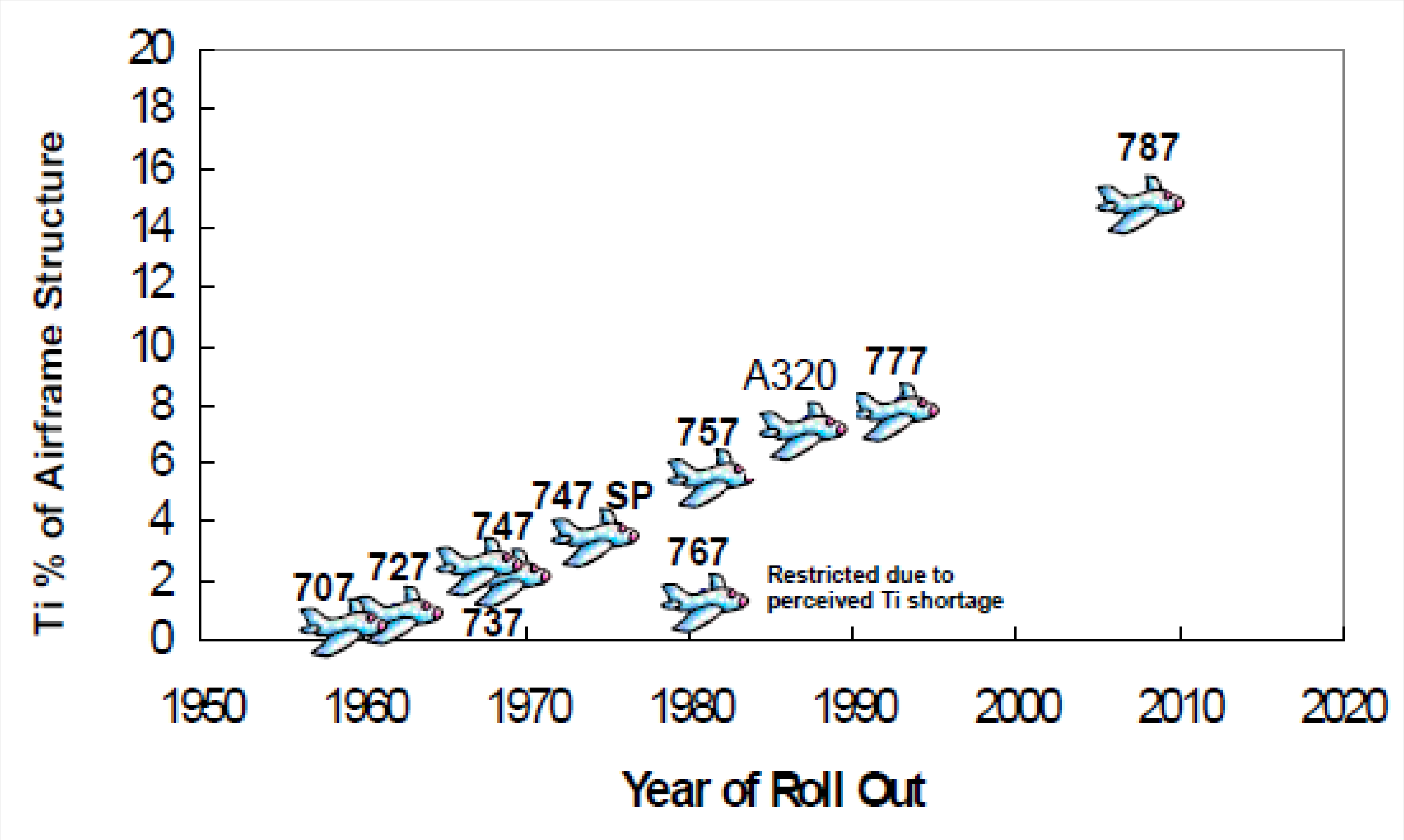

Titanium Value Chain—Forgings

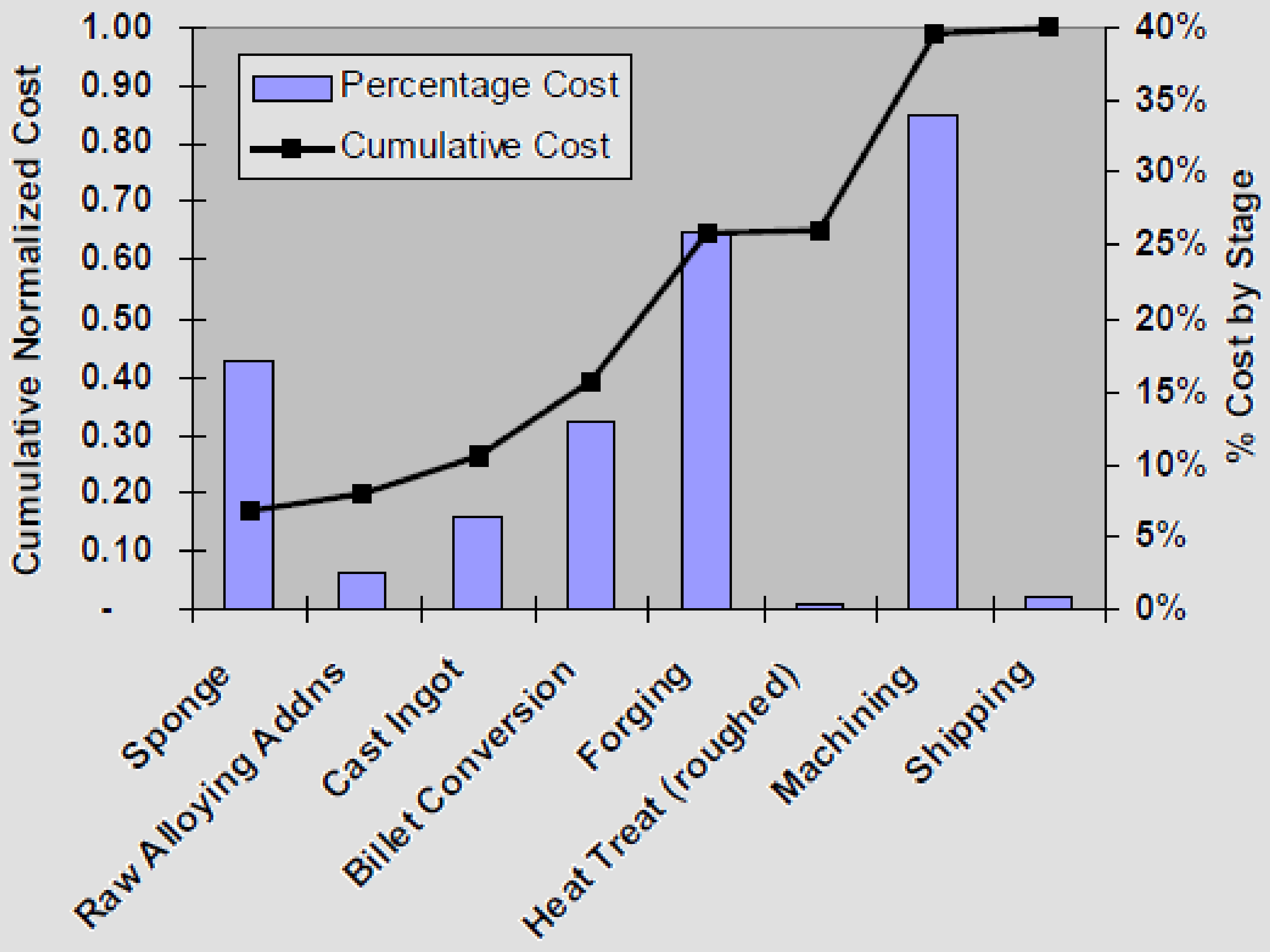

Titanium

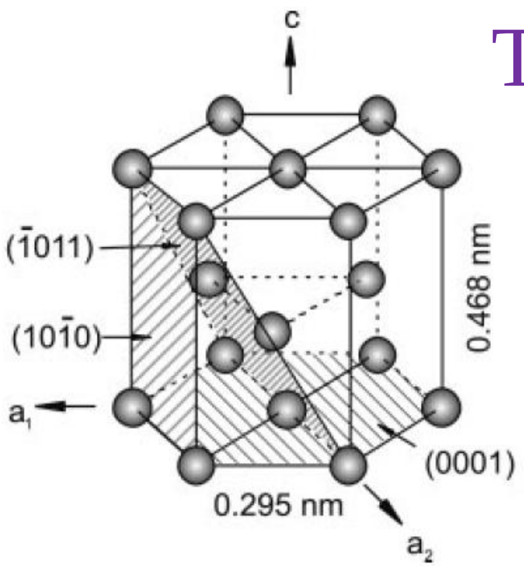

At 882°C

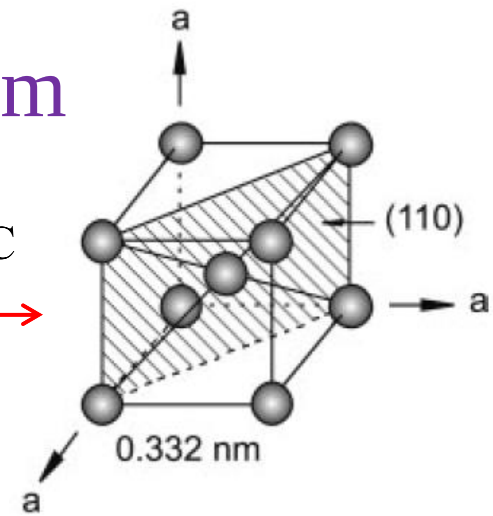

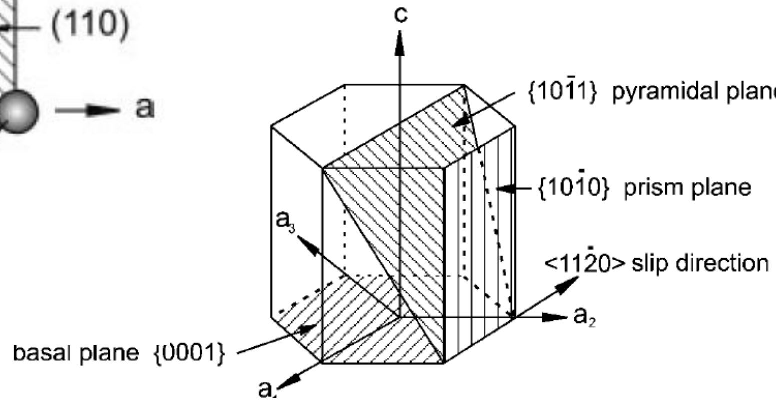

Effect of c/a Ratio on slip systems of HCP crystals

Typical slip systems observed in some HCP metals

Element	*c/a*	Deviation (%) from the ideal *c/a* = 1.633	Principal slip system	Secondary slip system	Other slip system
Cd	1.886	+15.5	Basal $\{0001\}\langle 11\bar{2}0\rangle$	Pyramidal $\{11\bar{2}2\}\langle 11\bar{2}3\rangle$	Prismatic $\{10\bar{1}0\}\langle 11\bar{2}0\rangle$ Pyramidal $\{10\bar{1}1\}\langle 11\bar{2}0\rangle$
Zn	1.856	+13.6	Basal $\{0001\}\langle 11\bar{2}0\rangle$	Pyramidal $\{11\bar{2}2\}\langle 11\bar{2}3\rangle$	Prismatic $\{10\bar{1}0\}\langle 11\bar{2}0\rangle$
Mg	1.624	−0.6	Basal $\{0001\}\langle 11\bar{2}0\rangle$	Prismatic $\{10\bar{1}0\}\langle 11\bar{2}0\rangle$	Pyramidal $\{10\bar{1}1\}\langle 11\bar{2}0\rangle\{11\bar{2}2\}\langle 11\bar{2}3\rangle$
Co	1.623	−0.6	Basal $\{0001\}\langle 11\bar{2}0\rangle$	None	None
Zr	1.593	−2.4	Prismatic $\{10\bar{1}0\}\langle 11\bar{2}0\rangle$	Basal $\{0001\}\langle 11\bar{2}0\rangle$	Pyramidal $\{10\bar{1}1\}\langle 11\bar{2}0\rangle\{11\bar{2}2\}\langle 11\bar{2}3\rangle$
Ti	1.588	−2.8	Prismatic $\{10\bar{1}0\}\langle 11\bar{2}0\rangle$	Basal $\{0001\}\langle 11\bar{1}0\rangle$	Pyramidal $\{1011\}\langle 11\bar{2}0\rangle\{11\bar{2}2\}\langle 11\bar{2}3\rangle$
Hf	1.581	−3.2	Prismatic $\{10\bar{1}0\}\langle 11\bar{2}0\rangle$	Basal $\{0001\}\langle 11\bar{2}0\rangle$	
Be	1.568	−4.0	Basal $\{0001\}\langle 11\bar{2}0\rangle$	Prismatic $\{10\bar{1}0\}\langle 11\bar{1}0\rangle$	Pyramidal $\{10\bar{1}1\}\langle 11\bar{2}0\rangle\{11\bar{2}2\}\langle 11\bar{2}3\rangle$

Ref:- Materials Chemistry and Physics 81 (2003) 11–26

Ti-6Al-4V alloy

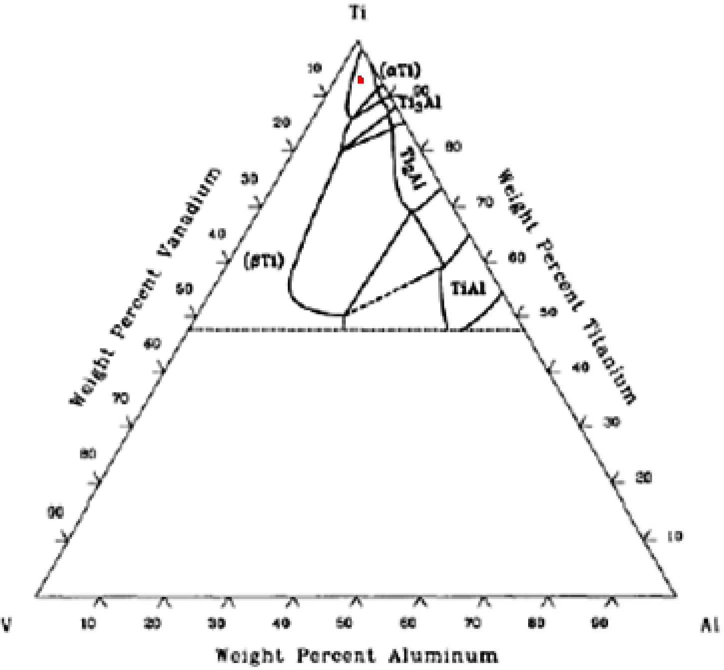

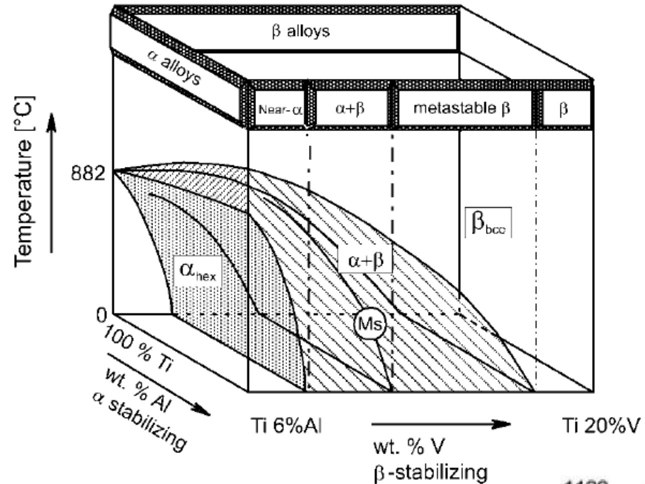

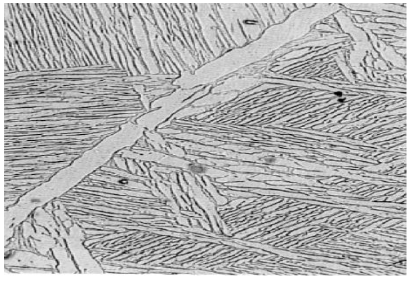

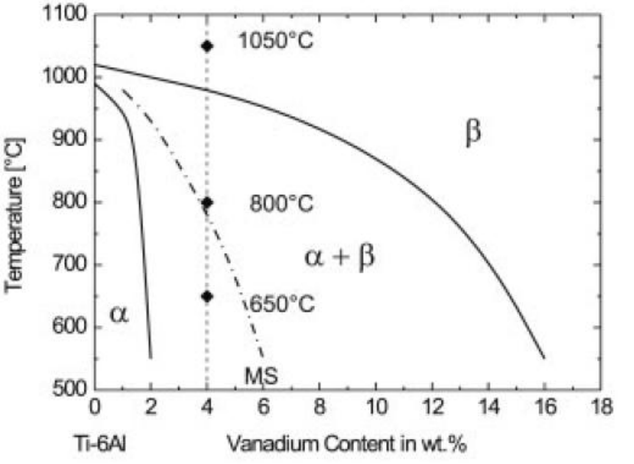

- At high cooling rate from above matensite start temp transform β phase completely into hcp α by diffusionless transformation
- It does not lead to embrittlement but slightly increased strength compared to α titanium
- Two types of matensite
  - Hexagonal α' matensite- shows needle like fine basket-weave structure
  - Orthorhombic α" martensite- quenching below 900˚C,shows good deformability

Ref:- Titanium and Titanium Alloys, C. Leyens and M. Peters,Wiley publication

The mechanics of machining

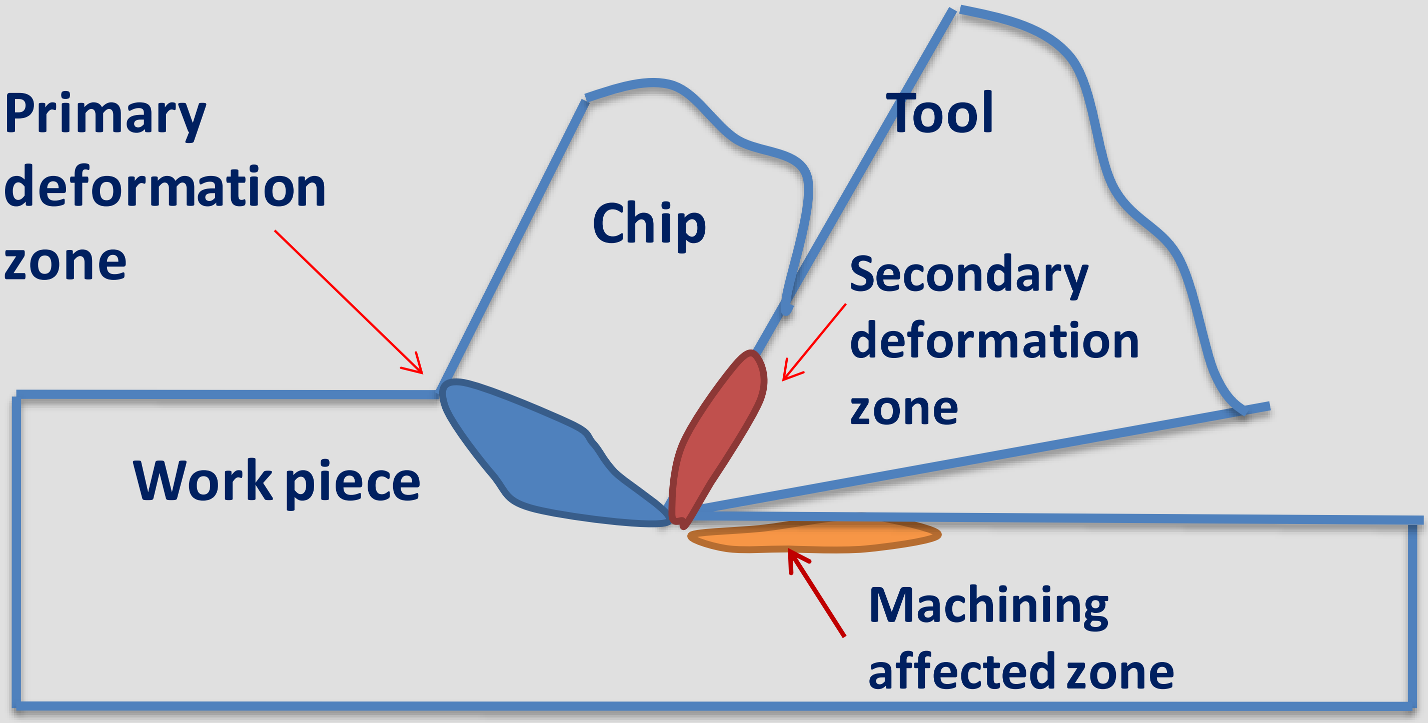

Chip freeze experiments

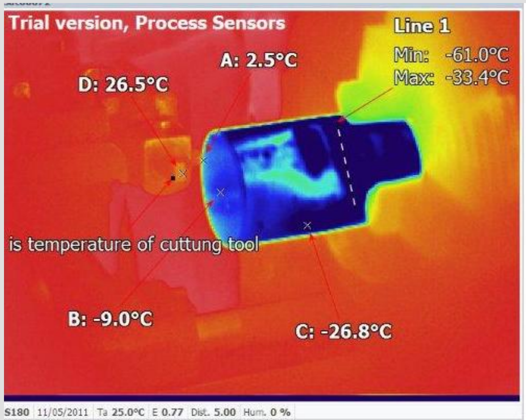

Temperature measurement

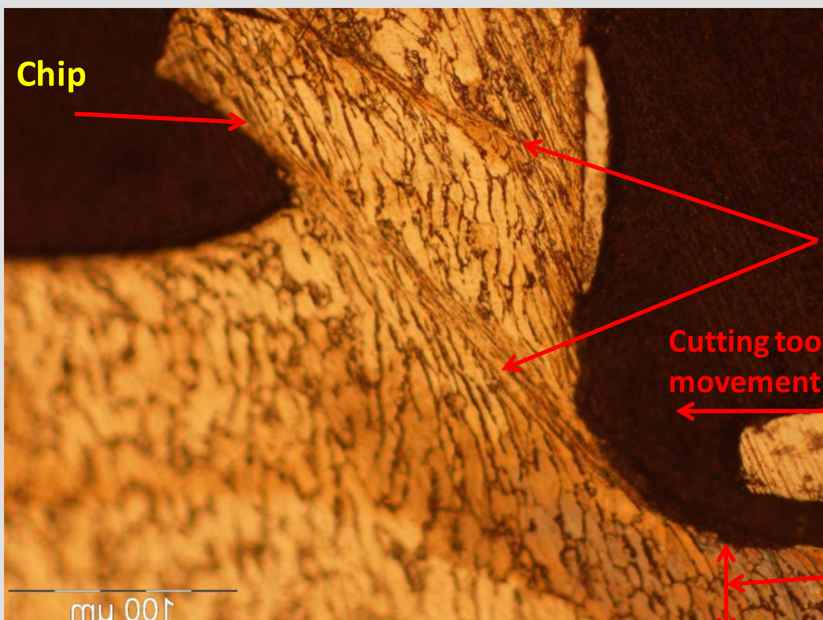

Adiabatic shear band

Machining affected surface

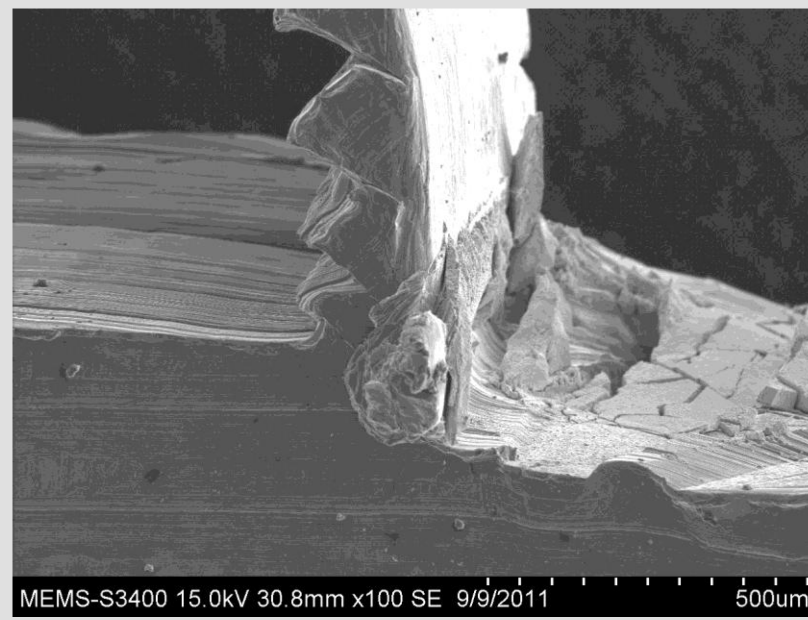

Chip microstructure at dry, LN2, elevated temperature machining condition

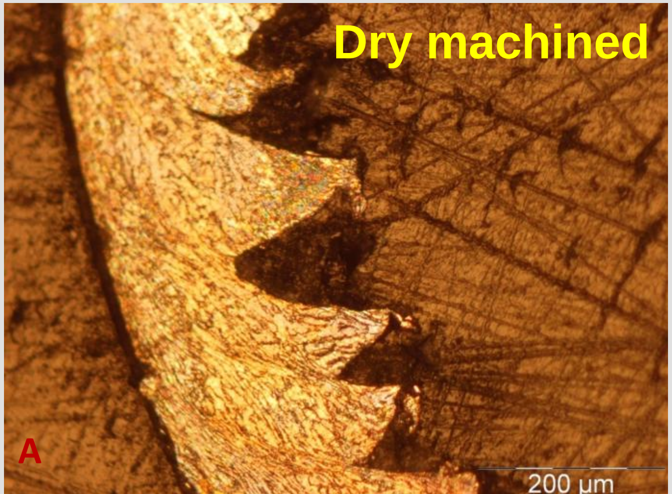

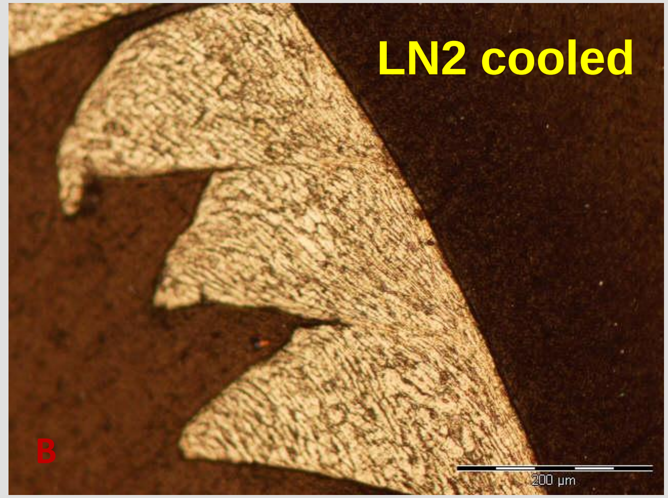

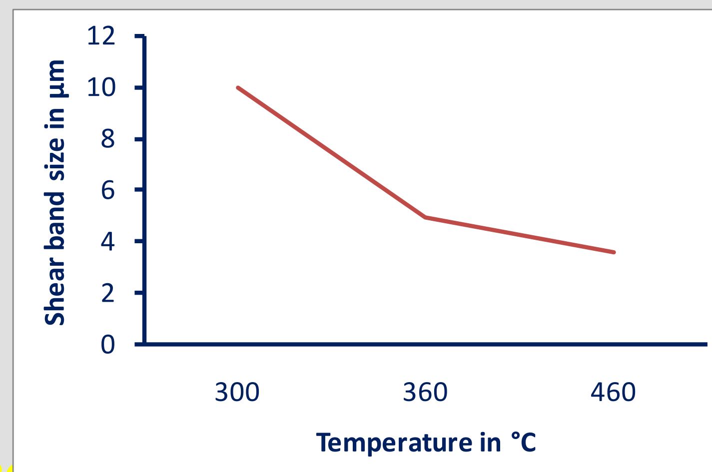

Increased machining affected zone(MAZ) and material is subjected higher strain rate with increased temperature

Machined edge

MAZ

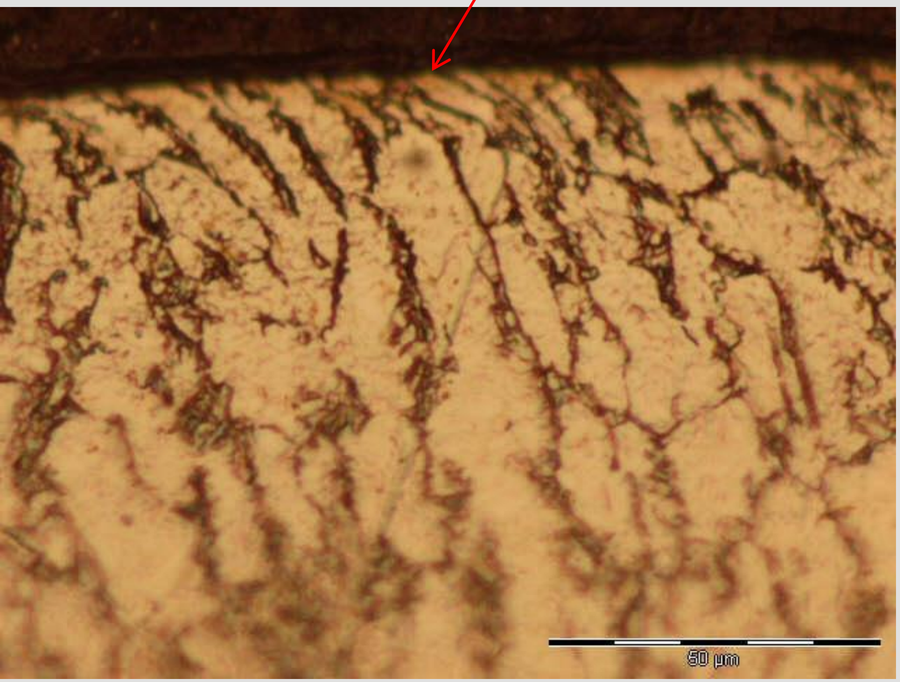

Optical image of chip obtained at 315 rpm
feed rate of 0.11 mm/rev at 350°C heating

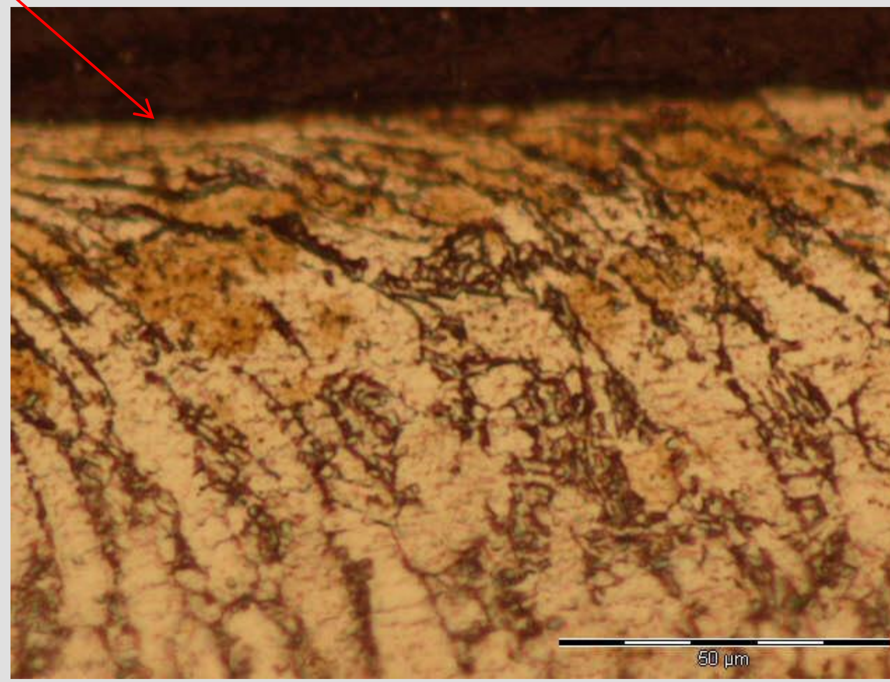

Optical image of chip obtained at 315 rpm
feed rate of 0.11 mm/rev at 500°C heating

Electron Back Scatter Diffraction of Machining affected zone

Machined edge

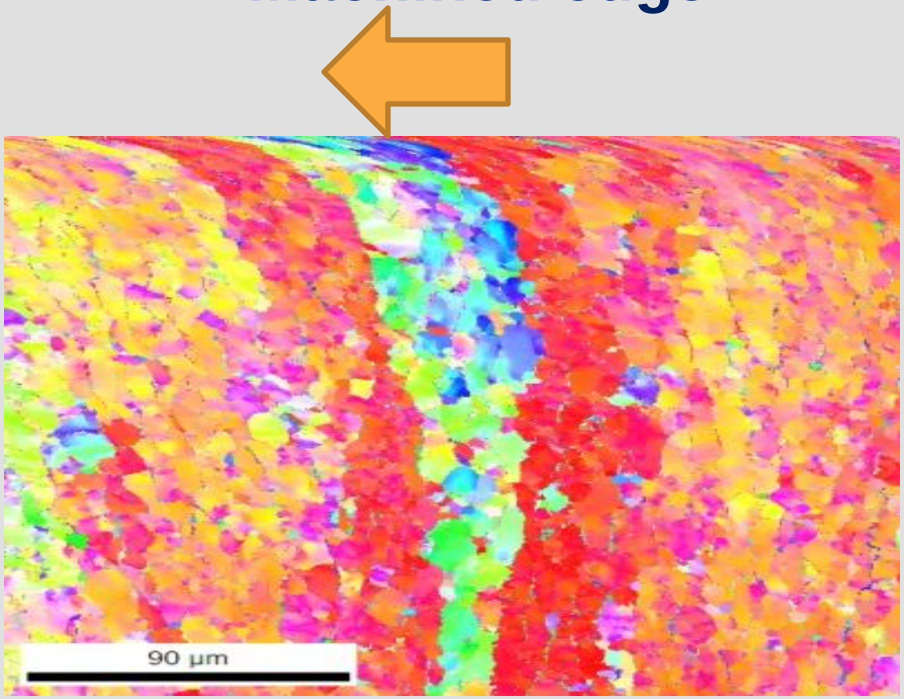

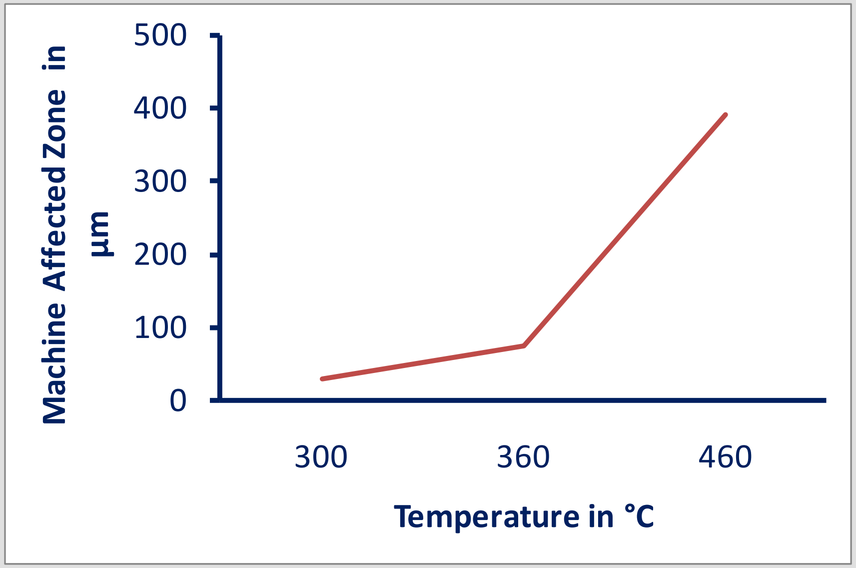

Influence of speed on residual stress at Machined edge

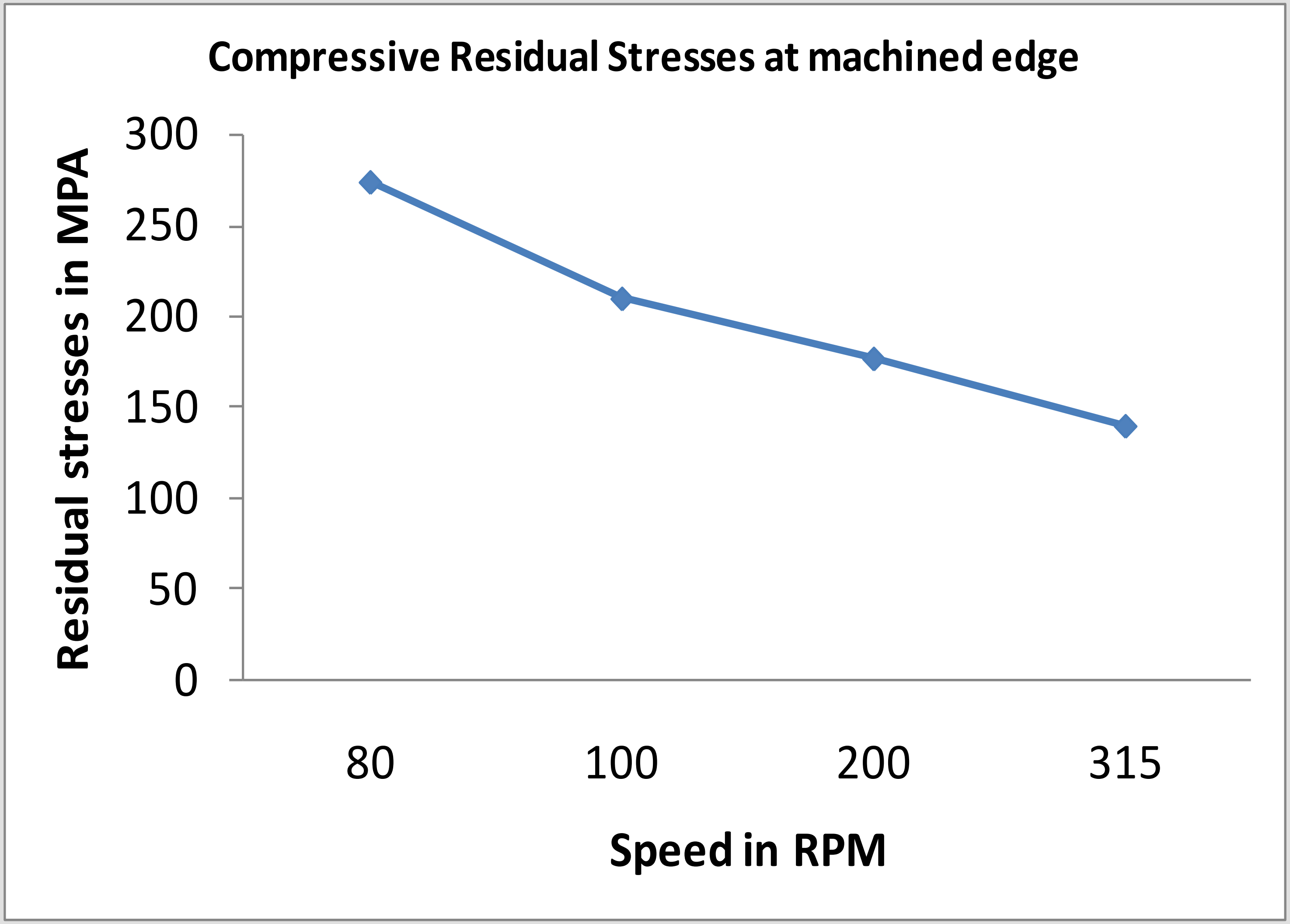

Influence of speed (feed constant 0.097 mm/rev.)on residual stress at Machined edge

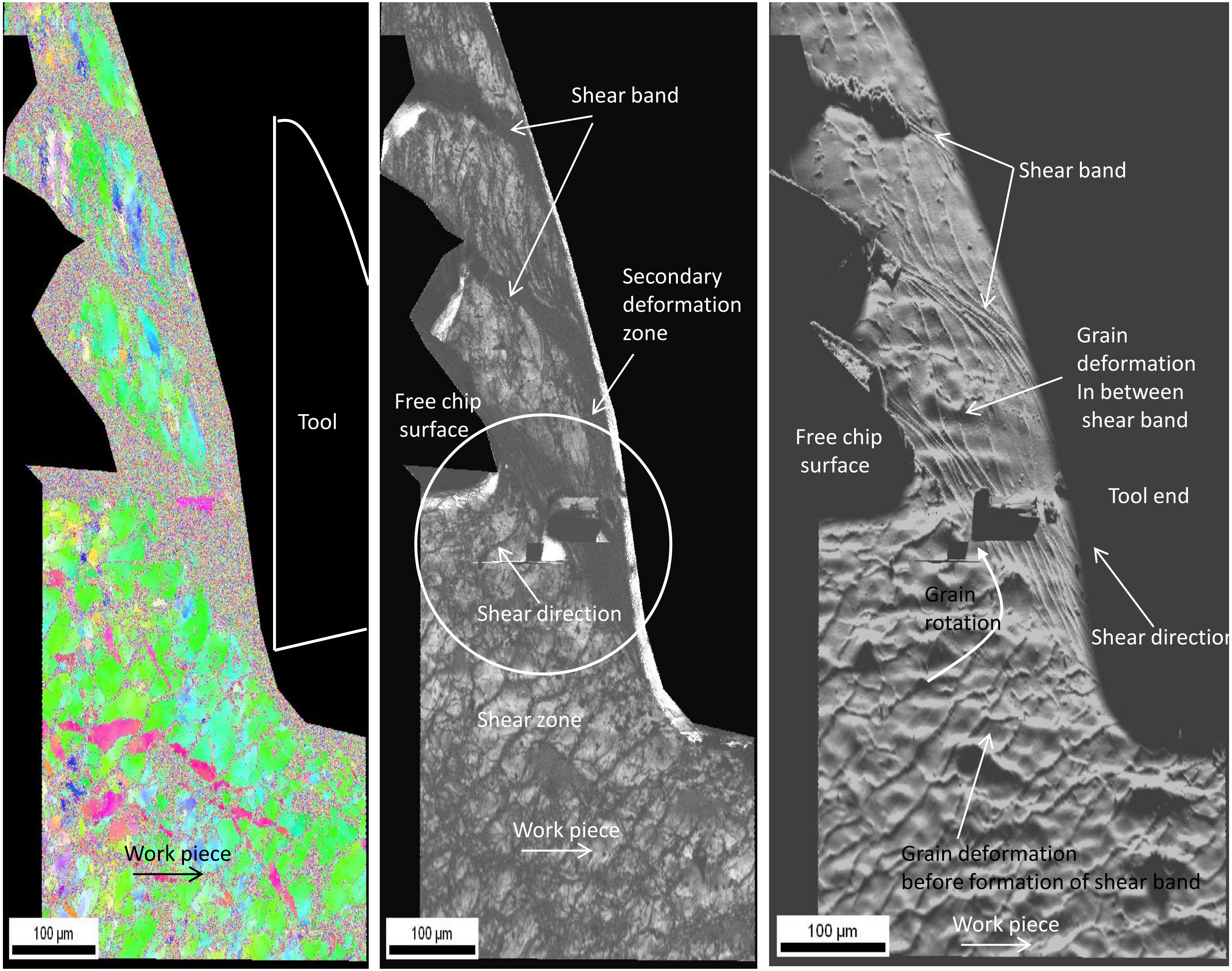

a. Phase quality map *b.* Image quality map *c.* SEM image

Fracture criteria

- Segmented chips even at low cutting speeds (saw tooth profile)
- Chip segmentation criteria
- ✓ Thermoplastic instability
- ✓ Initiation and propagation of cracks inside the primary shear zone of the workpiece material

Cockroft and Latham damage criterion: $C_i = \int_0^{\varepsilon_f} \sigma \left(\frac{\sigma^*}{\sigma}\right) d\varepsilon.$ [4,5,6]

Johnson Cook (JC) fracture model: $D = \sum \frac{\Delta\varepsilon}{\varepsilon_f}$ [7,8,9]

where, $\varepsilon_f = \left(D_1 + D_2 \exp(D_3 \sigma^*)\right)\left(1 + D_4 \ln\left(\frac{\dot{\varepsilon}}{\dot{\varepsilon}_0}\right)\right)\left(1 + D_5 \left(\frac{T - T_{room}}{T_{melt} - T}\right)^m\right)$ $\sigma^* = \frac{\sigma_m}{\sigma_v}$

Ref [4]"*Prediction of chip morphology and segmentation during the machining of titanium alloys*", Jiang Hua, Rajiv Shivpuri, Journal of Materials Processing Technology 150 (2004) 124–133

Ref [5] "*Finite element simulation of conventional and high speed machining of Ti6Al4V alloy*", Domenico Umbrello, Journal of materials processing technology 196 (2008) 79–87

Ref [6]"*FEM simulation of orthogonal cutting: serrated chip formation*", E. Ceretti, M. Lucchi, T. Altan, Journal of Materials Processing Technology 95 (1999) 17-26

Ref[7]"*Material flow stress and failure in multiscale machining titanium alloy Ti-6Al-4V*", J. Sun & Y. B. Guo, Int J Adv Manuf Technol (2009) 41:651–659

Ref[8]"*A contribution to a qualitative understanding of thermo-mechanical effects during chip formation in hard turning*", T. Mabrouki , J.-F. Rigal, Journal of Materials Processing Technology 176 (2006) 214–221

Ref [9]"*Modelling of hard part machining*", Eu-Gene Ng, David K. Aspinwall, Journal of Materials Processing Technology 127 (2002) 222–229

Material Models

JC Model $\sigma = (A + B\varepsilon^n)\left(1 + C \cdot \ln\left(\frac{\dot{\varepsilon}}{\dot{\varepsilon}_o}\right)\right)\left(1 - \left(\frac{T - T_{room}}{T_{melt} - T}\right)^m\right)$	Takes in to account strain hardening effect, viscosity effect softening effect.	Coupling effects of strain rate and temperature absent The parameters fitted to the stress–strain curves (SPHB)
Modified JC model $\sigma = \left(A + B\varepsilon^n\left(\frac{1}{\exp(\varepsilon^a)}\right)\right)\left(1 + C \cdot \ln\left(\frac{\dot{\varepsilon}}{\dot{\varepsilon}_o}\right)\right)\left(1 - \left(\frac{T - T_{room}}{T_{melt} - T}\right)^m\right)\left(D + (1 - D)\tanh\left(\frac{1}{(\varepsilon + s)^c}\right)\right)$	Incorporates the strain softening effect Was able to account for segmented chips formation at low cutting speed	The above mentioned models do not consider the effect of microstructure during machining.
Micromechanical Physic based model $\sigma = (1215 \cdot \varepsilon^{0.06}) + 601.2\left(\left(1 - \left(-9.58X10^{-5}T.\ln\left(\frac{\dot{\varepsilon}}{4.2X10^8}\right)\right)^{\frac{4}{5}}\right)\right)^{\frac{3}{4}}$	Flow stress has two parts: Athermal part (σ_a) Thermal part (σ^*)	Above critical temperature, gave a constant value of stress for all temperature hence not for machining
Modified Micromechanical physics based model $\sigma = (a\varepsilon^n + b)(cT^{*2} + dT^* + e)h(\varepsilon, \dot{\varepsilon})$	Temperature dependent flow softening	Phase change not incorporated.

FEM Simulation

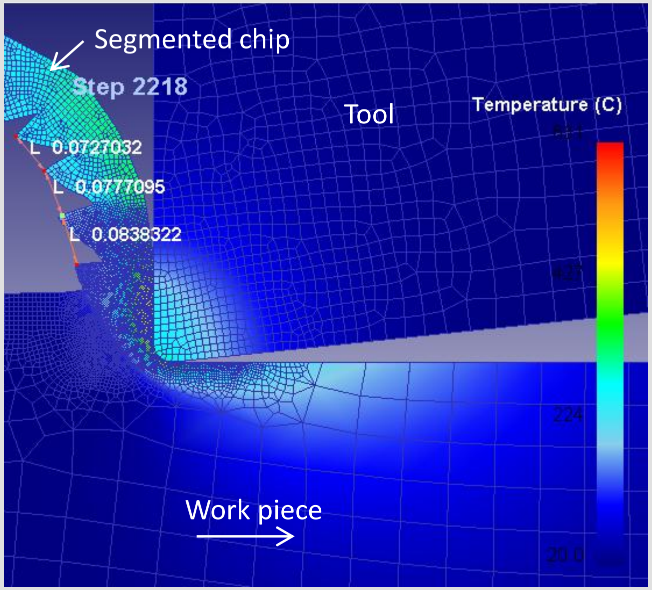

a. at 23.4 m/min , room temp.

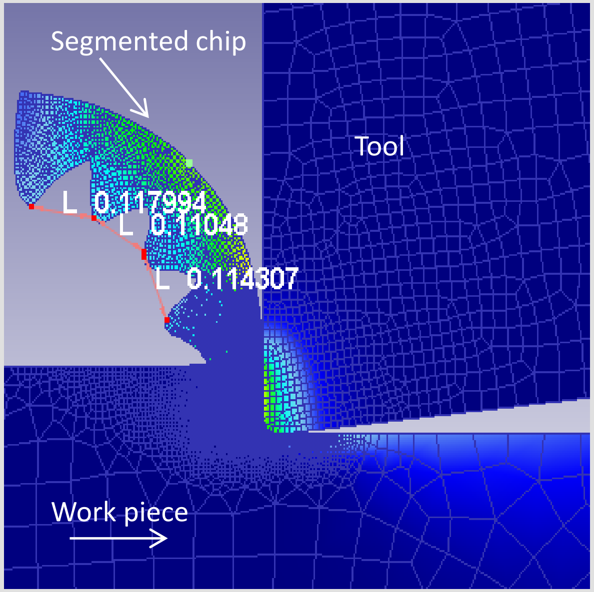

b. at 91.8 m/min, room temp.

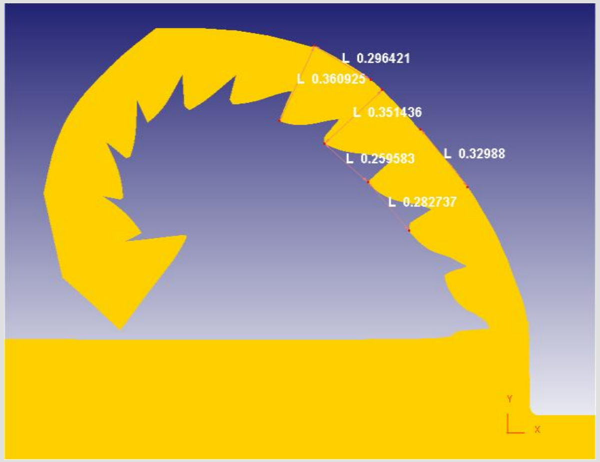

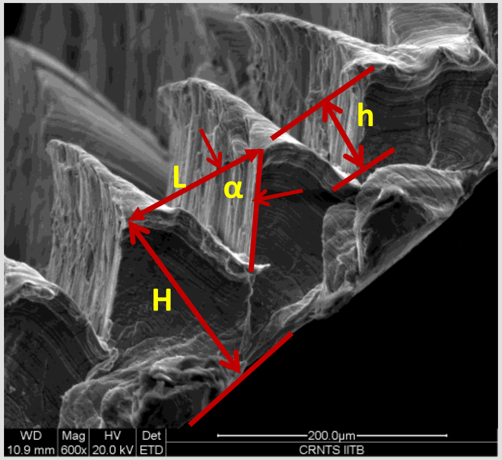

Phase transformation calculation

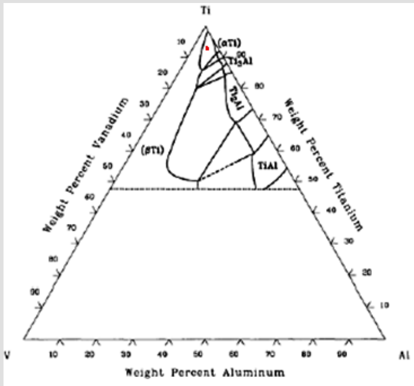

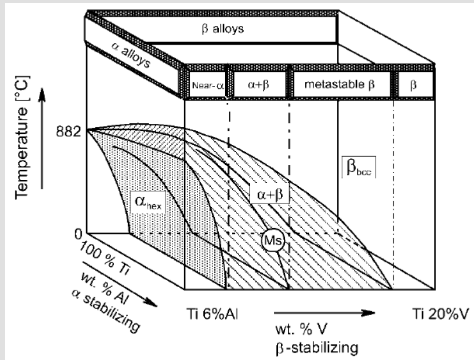

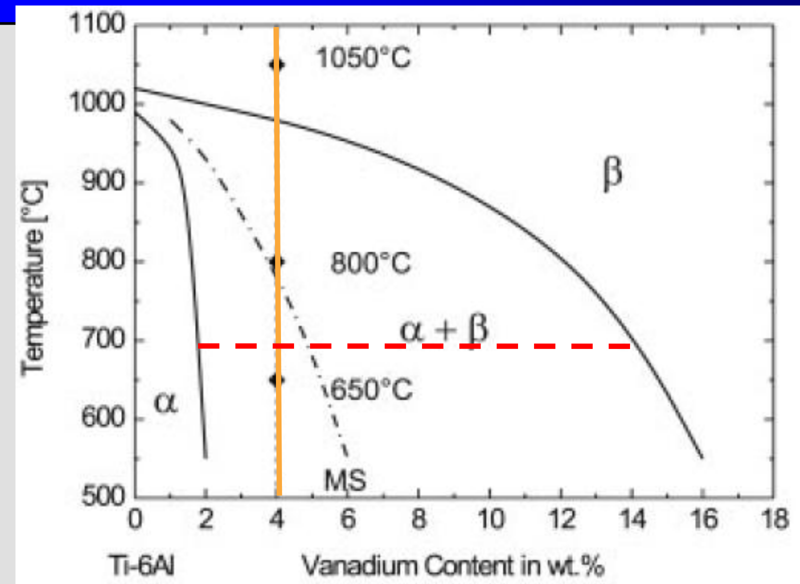

Temperature distribution
20 deg C (130) To 700 deg C (254)

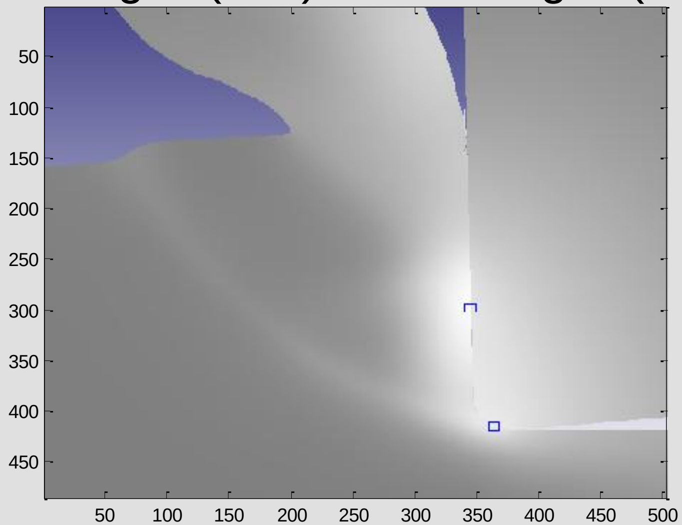

Beta Phase distribution
8% (0) To 20% (255)

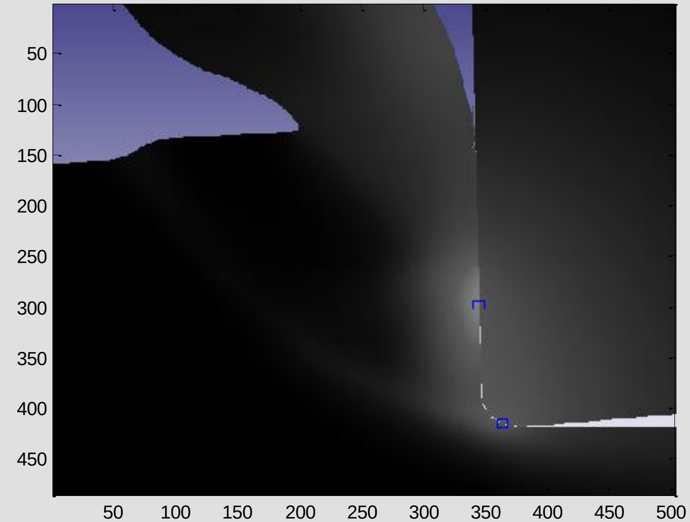

Case Study 2

Aluminum sheet metal forming

Motivation

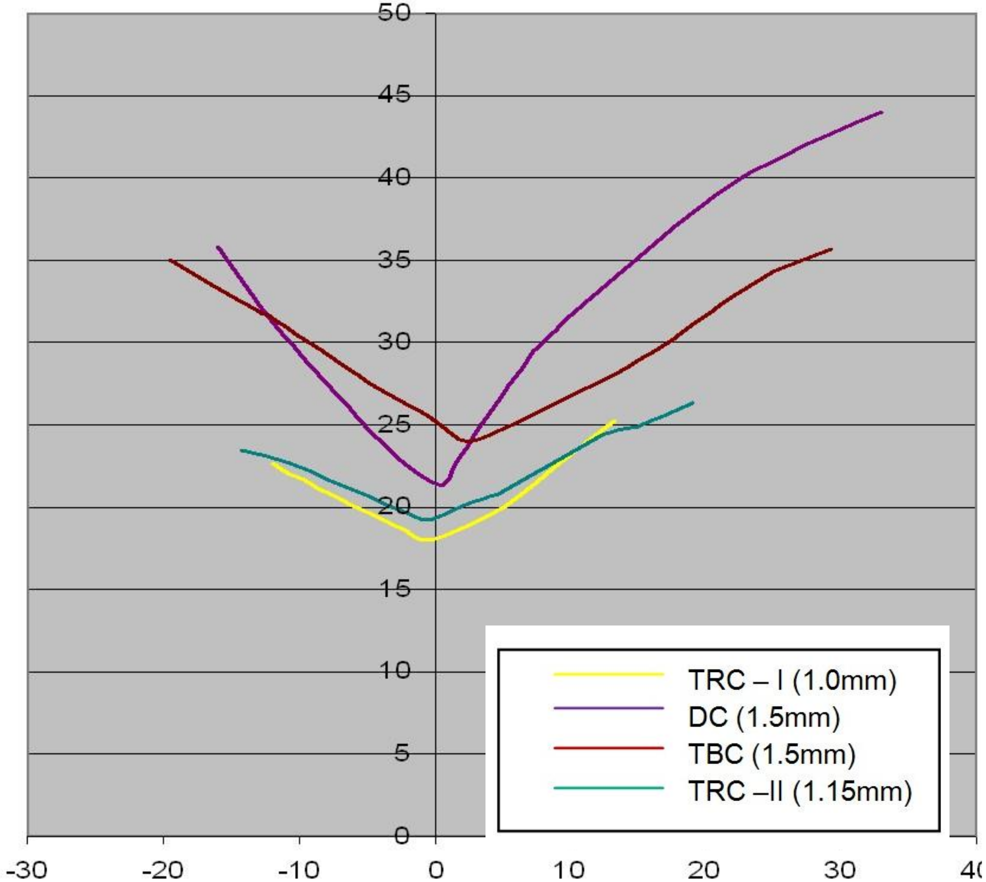

Large formability variation of same 5754 Al alloy processed through different processes

Alloy composition and processing

5754 Alloy	Mg wt%	Mn wt%	Cr wt%	Fe wt%	Si wt%
DC	3.0	0.25	0.01	0.18	<0.10
TBC	3.1	0.25	<0.01	0.24	<0.10
TRC-I	2.8	0.01	<0.01	0.25	0.10
TRC-II	2.9	0.01	<0.01	0.24	0.08

Di

Co

Co

Typical microstructure of various 5754 alloys

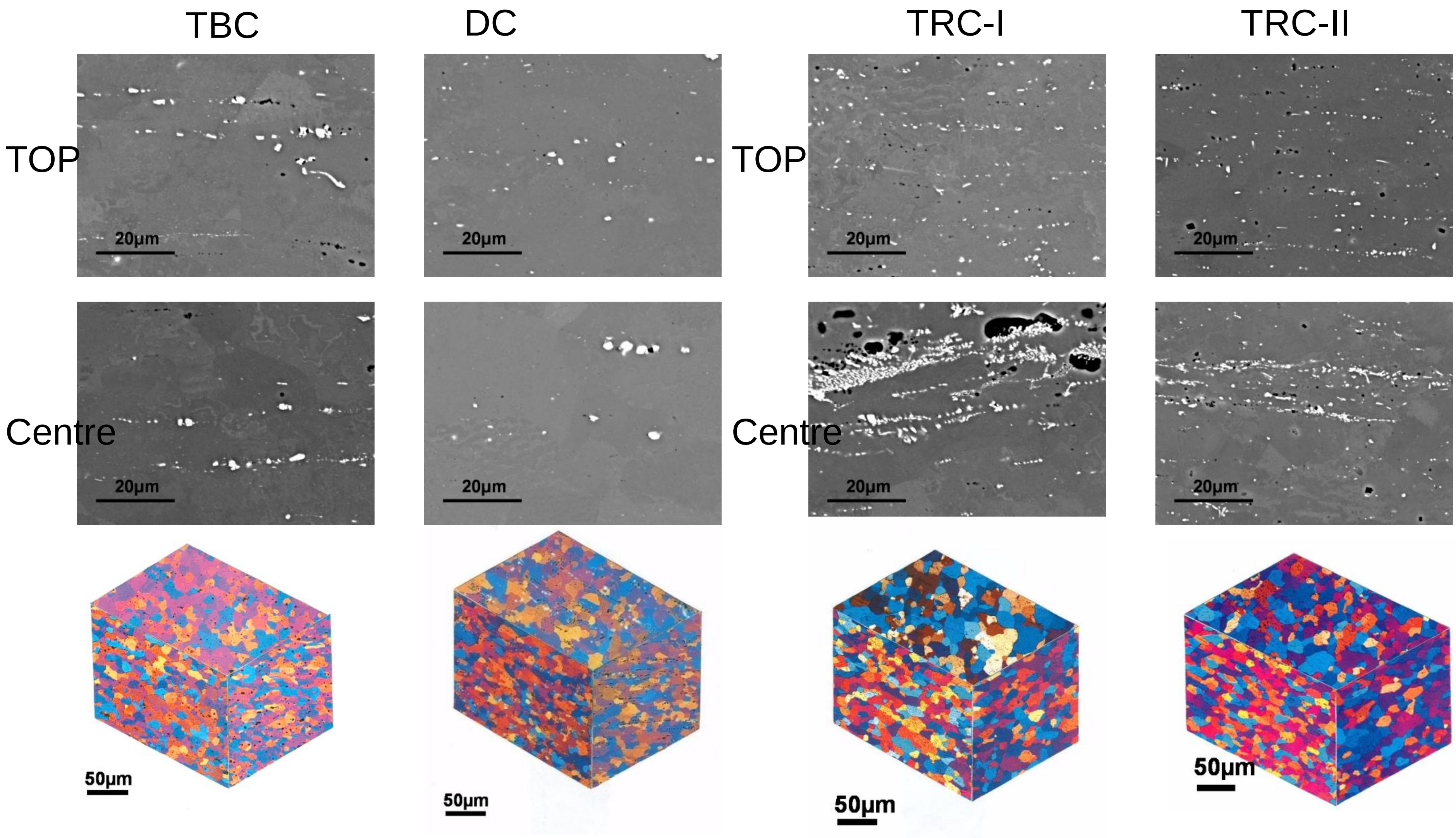

Center-line Segregation

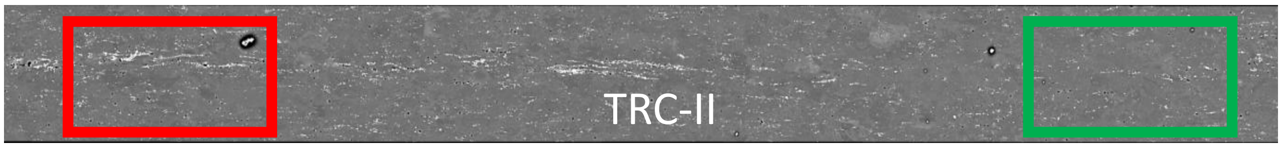

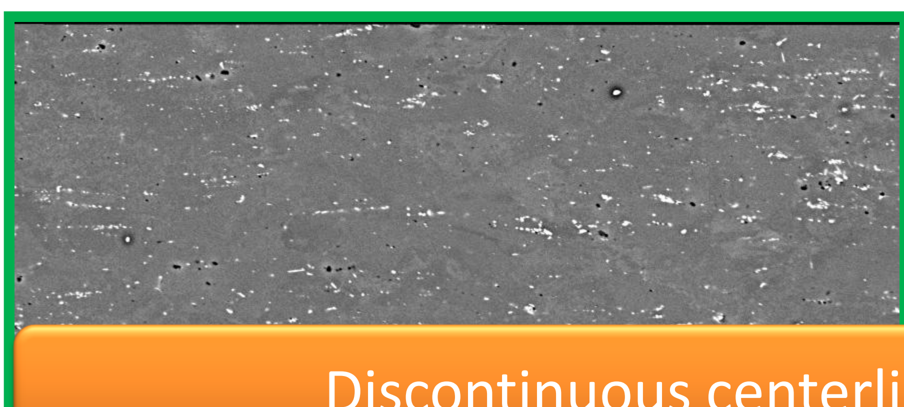

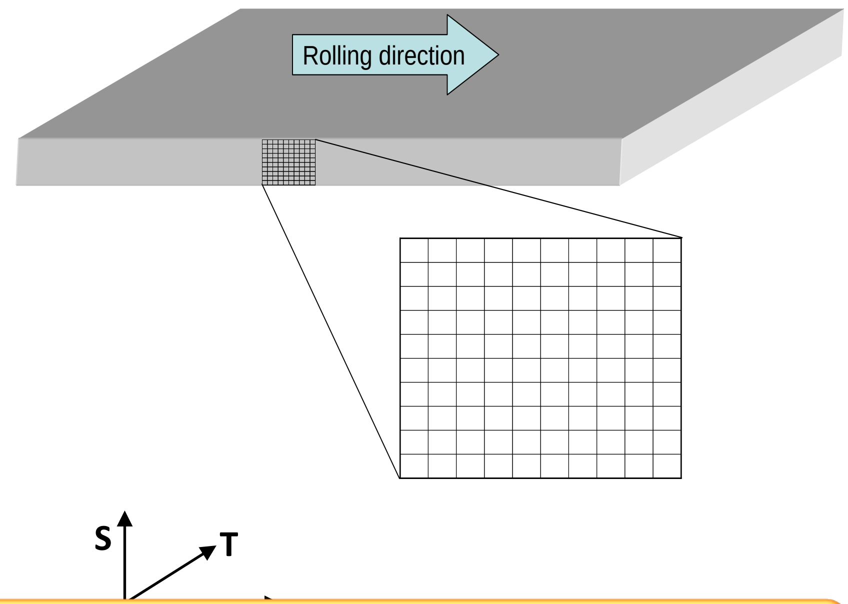

Discontinuous centerline segregation in TRC-II

Second phase particles

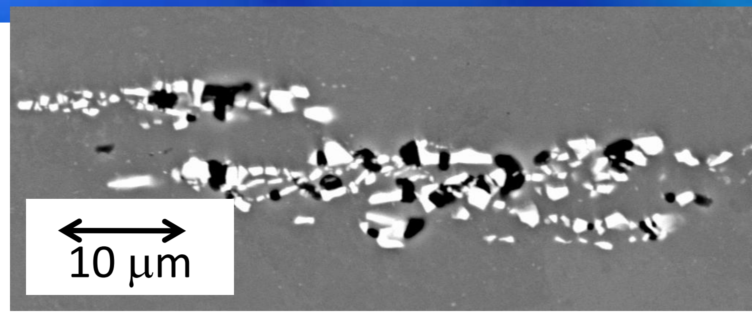

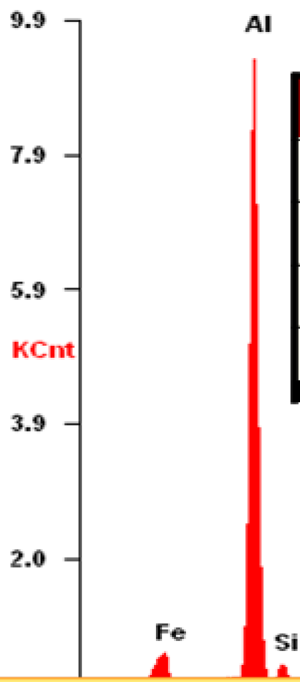

Element	Wt%	At%
AlK	70.75	81.03
SiK	04.95	05.44
MnK	07.93	04.46
FeK	16.37	09.06

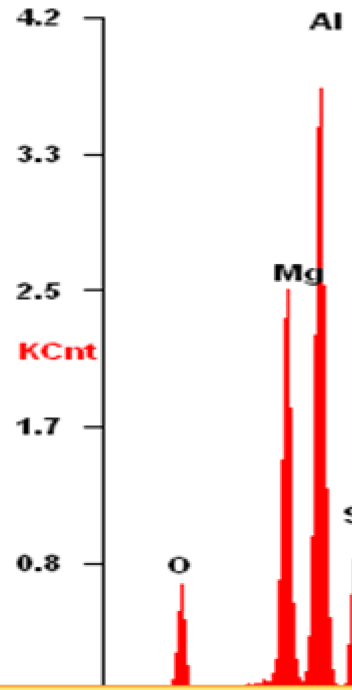

Element	Wt%	At%
O K	13.96	21.16
MgK	21.53	21.47
AlK	47.48	42.67
SiK	17.03	14.71

Two type of second phase particles are present

Through thickness microstructure variation

	Intermetallics		Oxides	
	Volume fraction	Size (μm)	Volume fraction	Size (μm)
DC	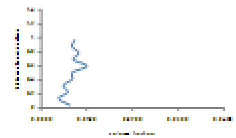	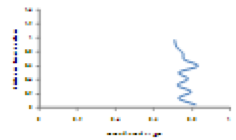	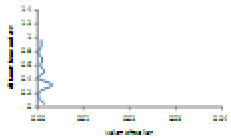	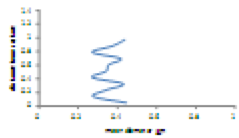
TBC	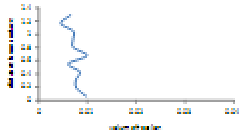	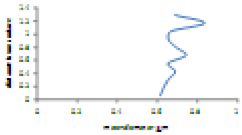	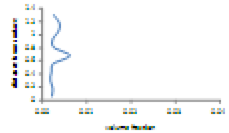	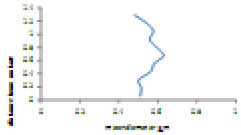
TRC - I	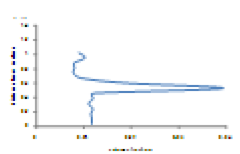	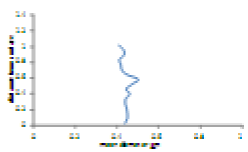	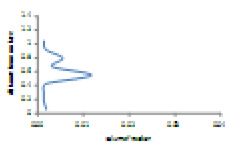	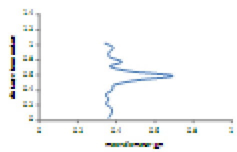
TRC - II	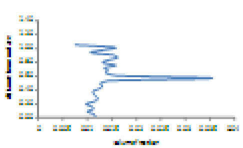	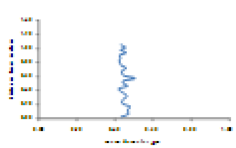	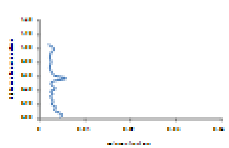	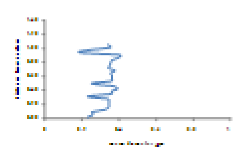

Mechanical properties along the rolling direction

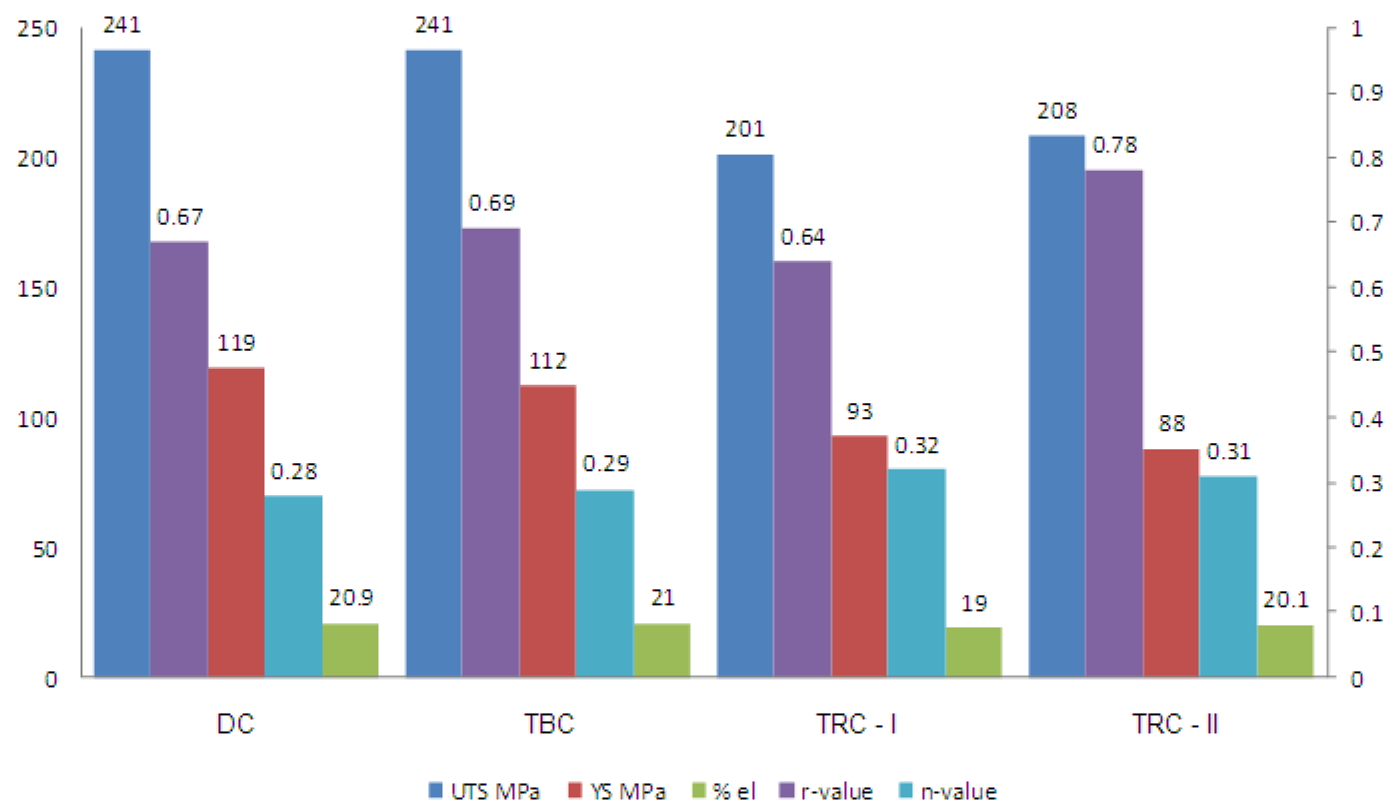

TRC has lower YS and UTS than TBC or DC

Fractographic investigation (TRC-I)

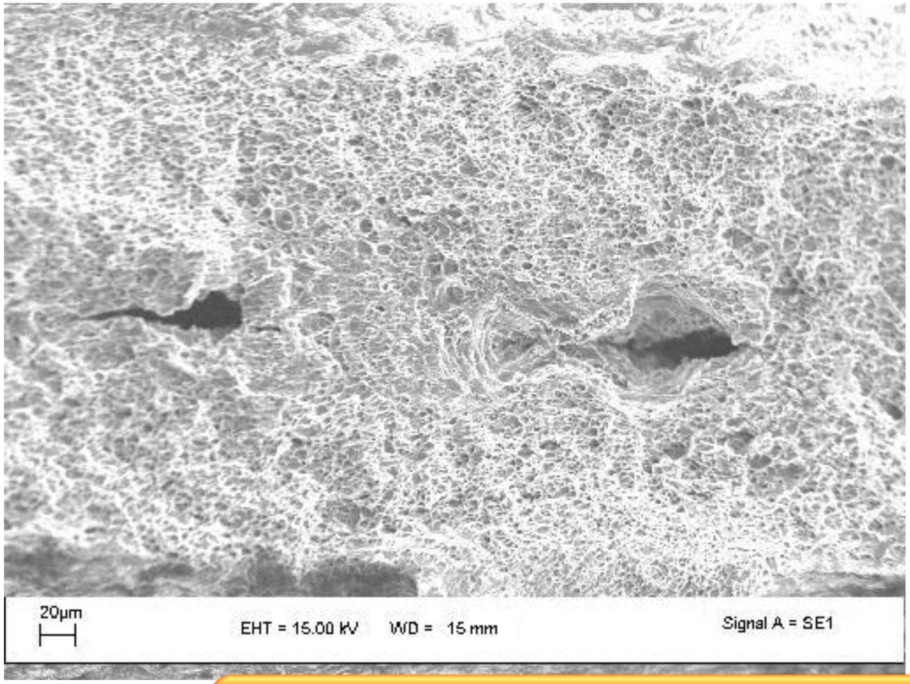

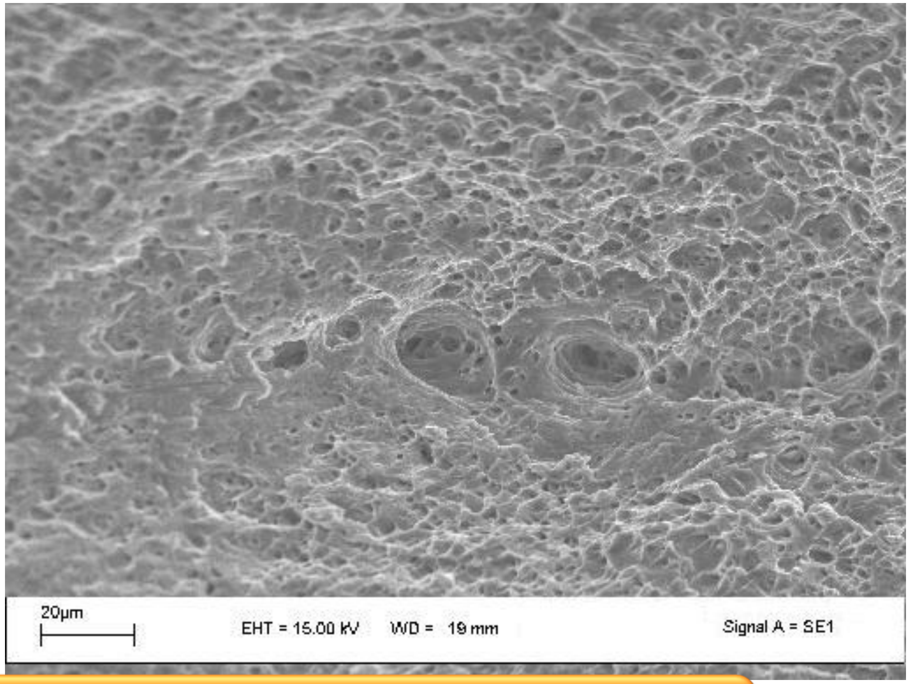

Microvoid formation at particle clusters

Microstructure based FEA

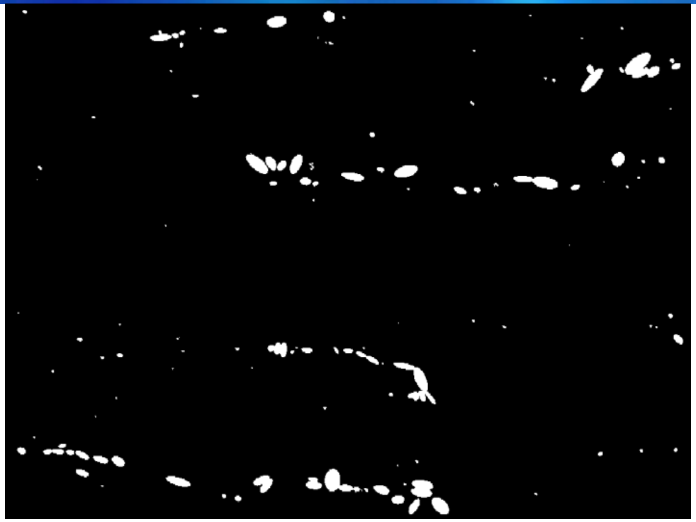

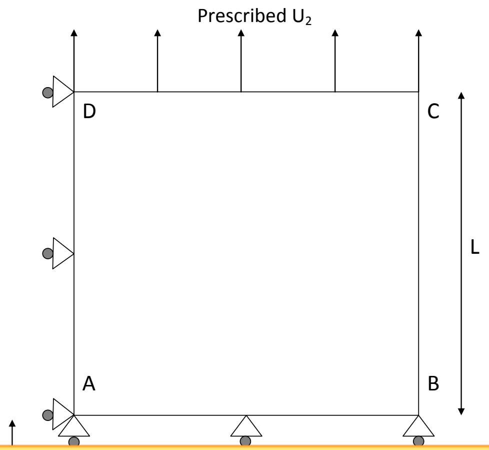

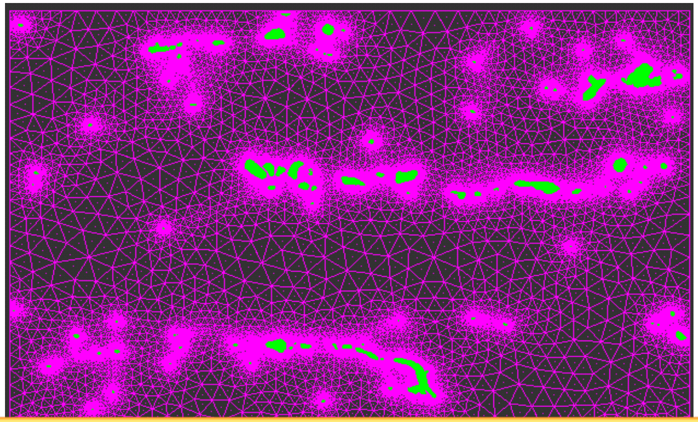

Modeling particles as intersecting ellipses is a good approximation

FE predictions of uniaxial stress-strain behavior

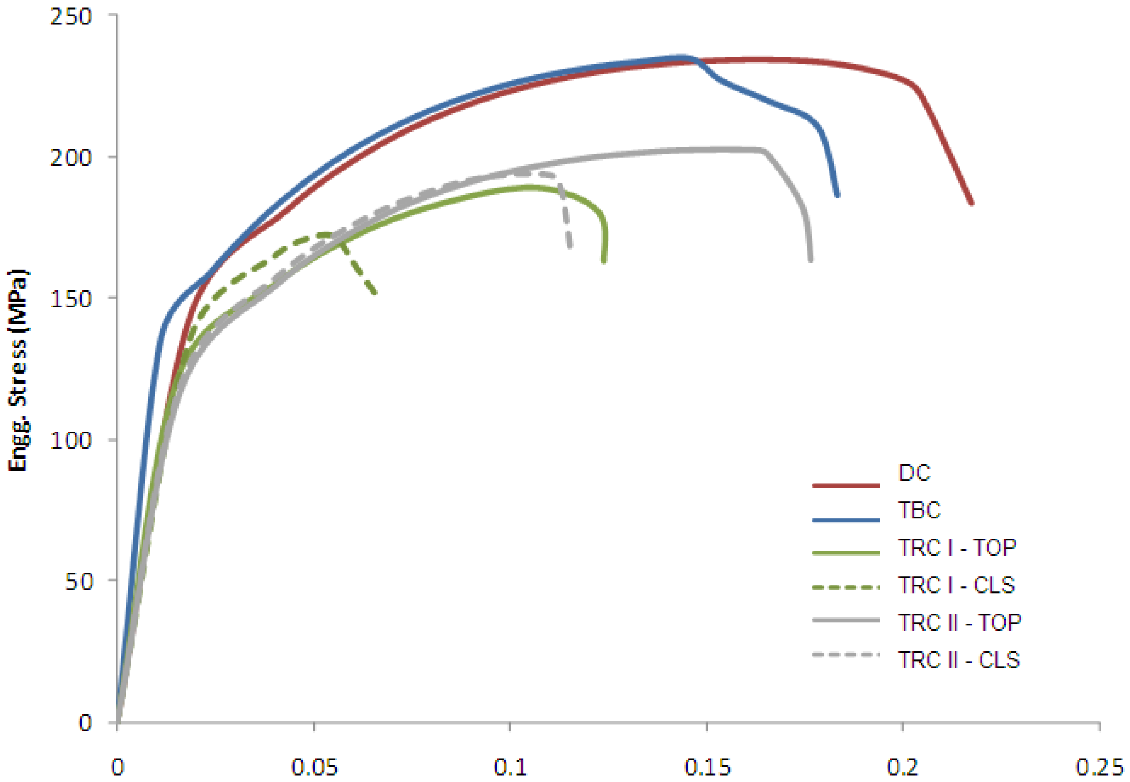

Novelis has higher localization strain than Assan

With in Assan, center region has lower localization strain than top

Correlation of localization strain and Extreme Property Index (EPI)

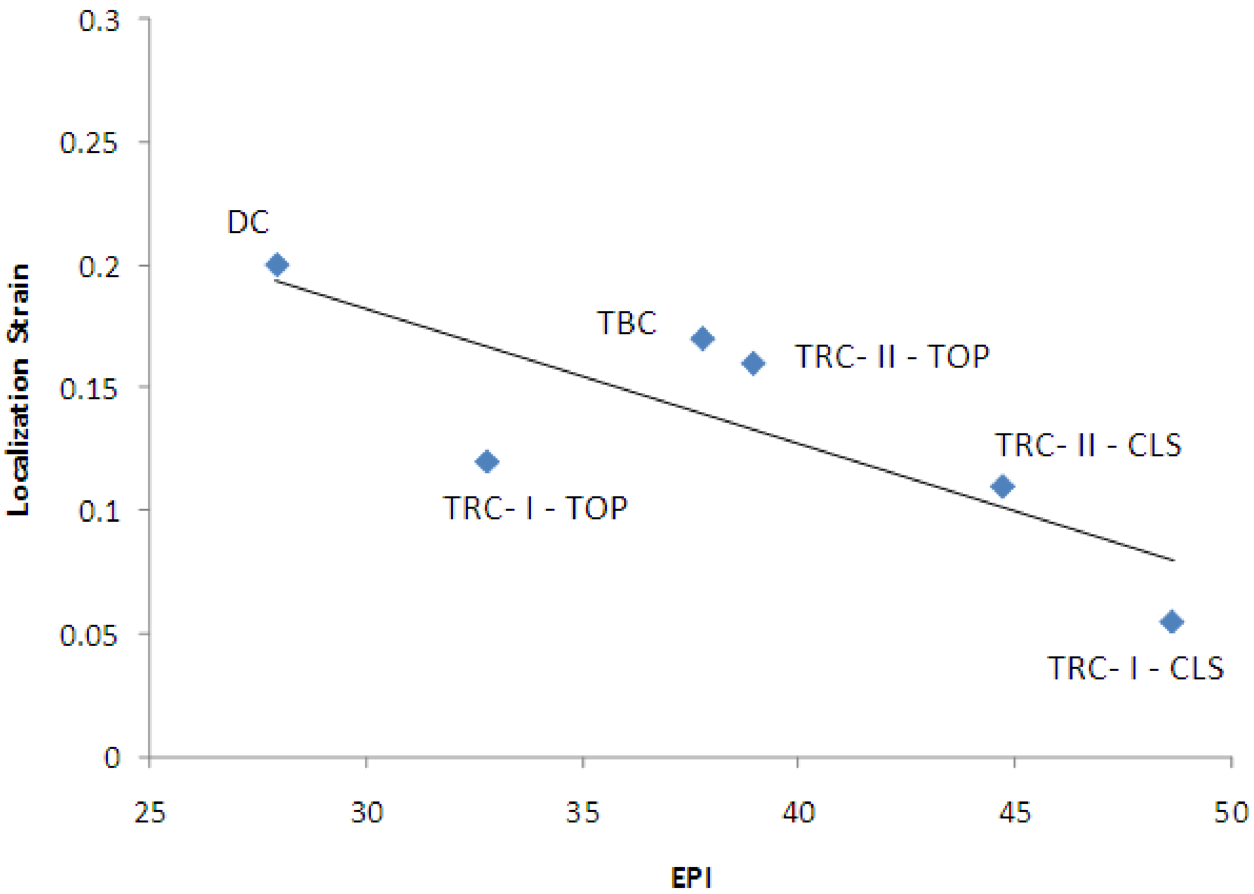

EPI is identified as a key microstructural attribute

Plastic deformation by slip

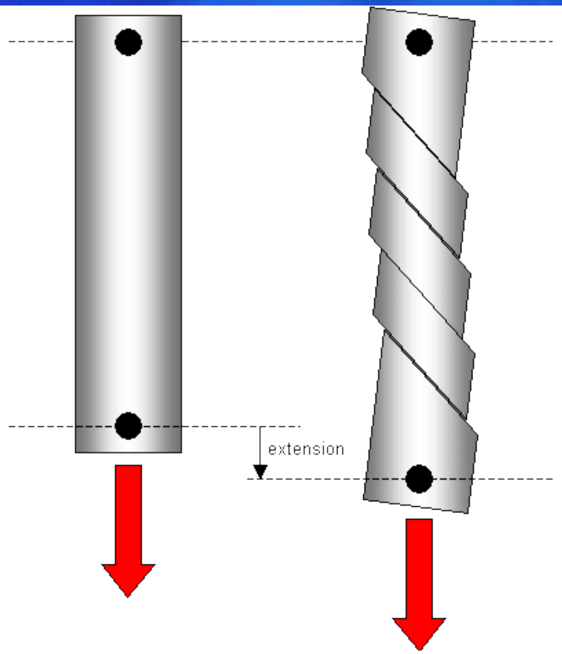

Unslipped single crystal fixed at top end.

Single crystal after plastic deformation by tensile stress in the direction of the arrow. Slip occurs on distinct parallel

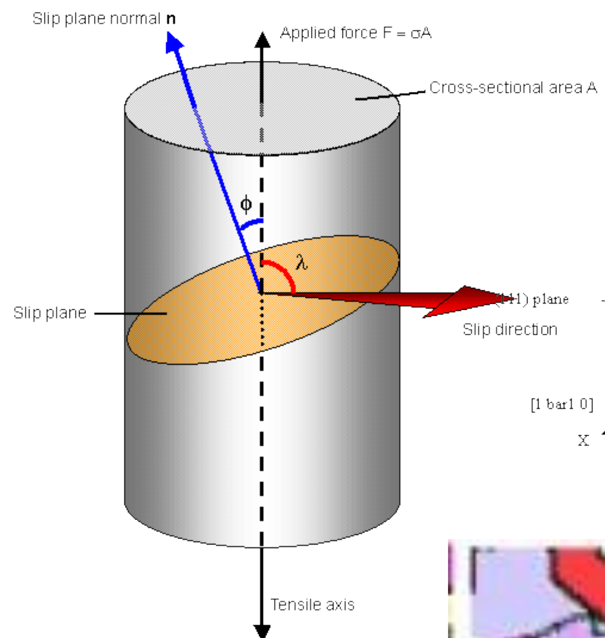

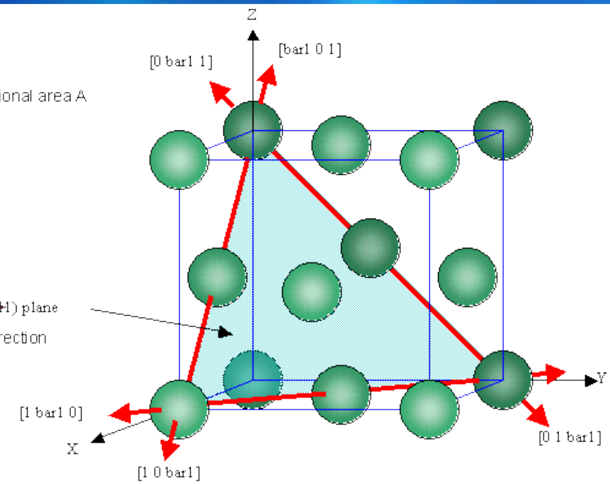

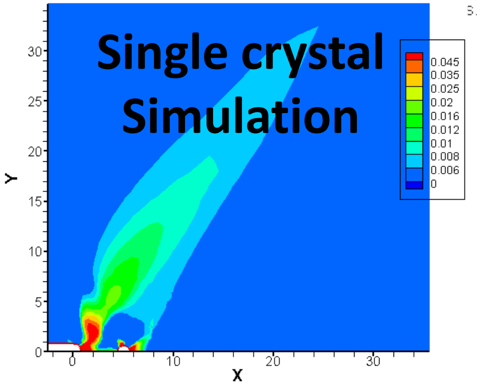

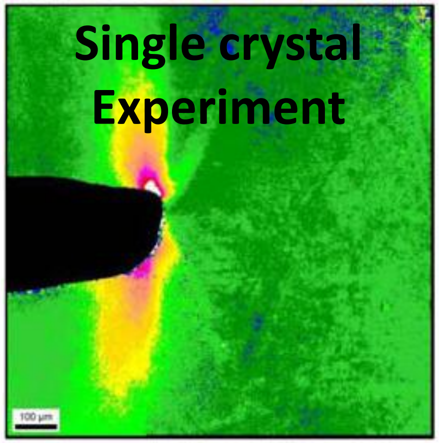

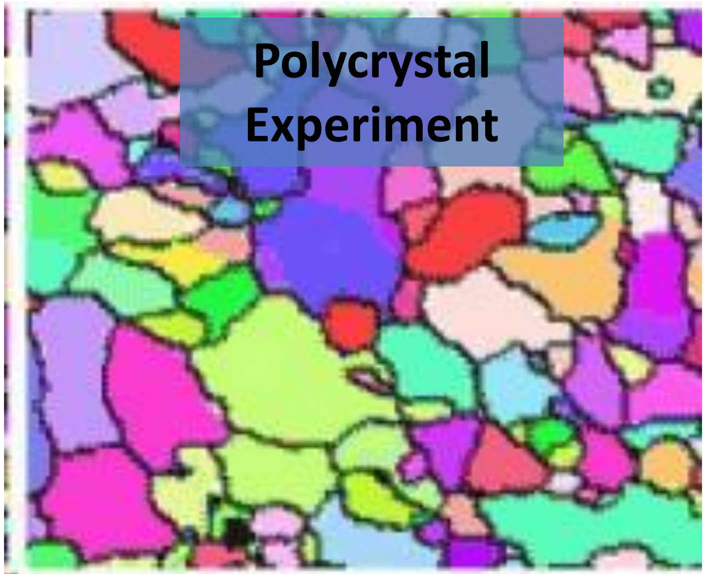

Inverse pole figure maps

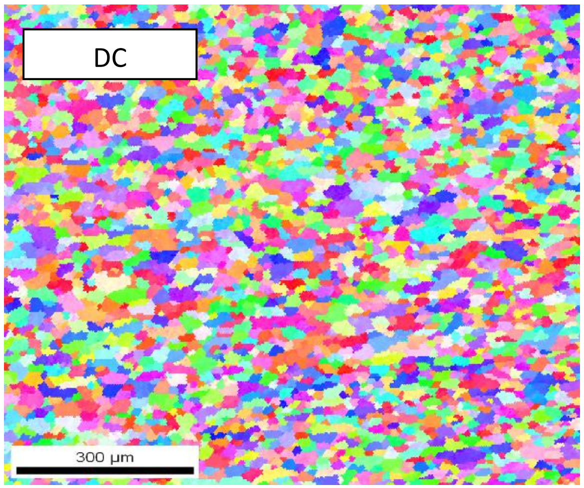

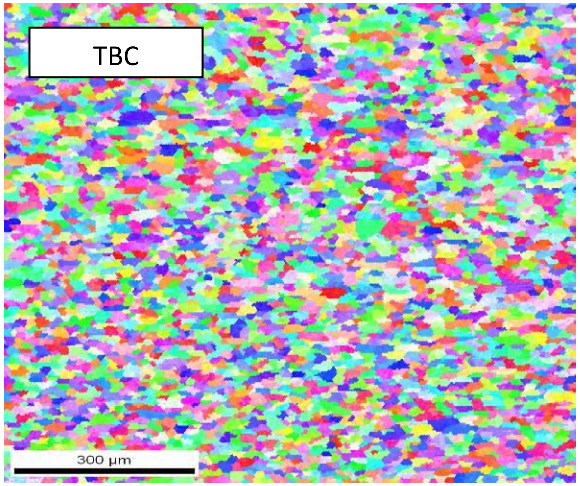

Rolling Direction

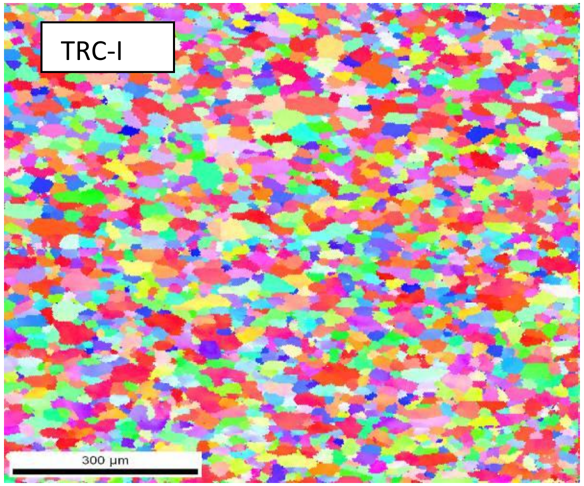

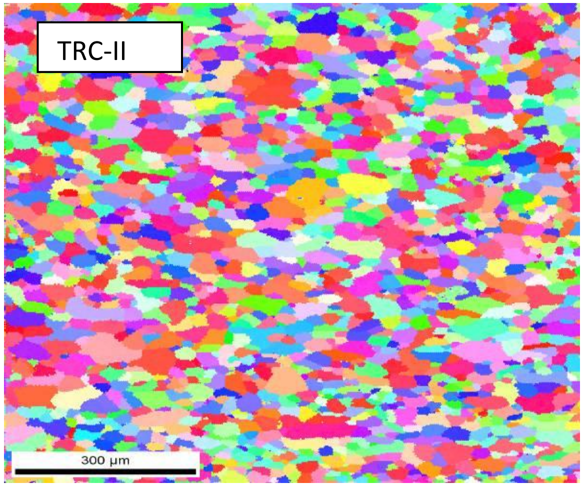

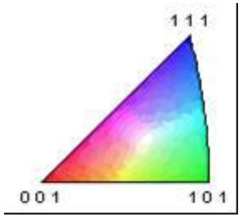

Fraction of various texture components

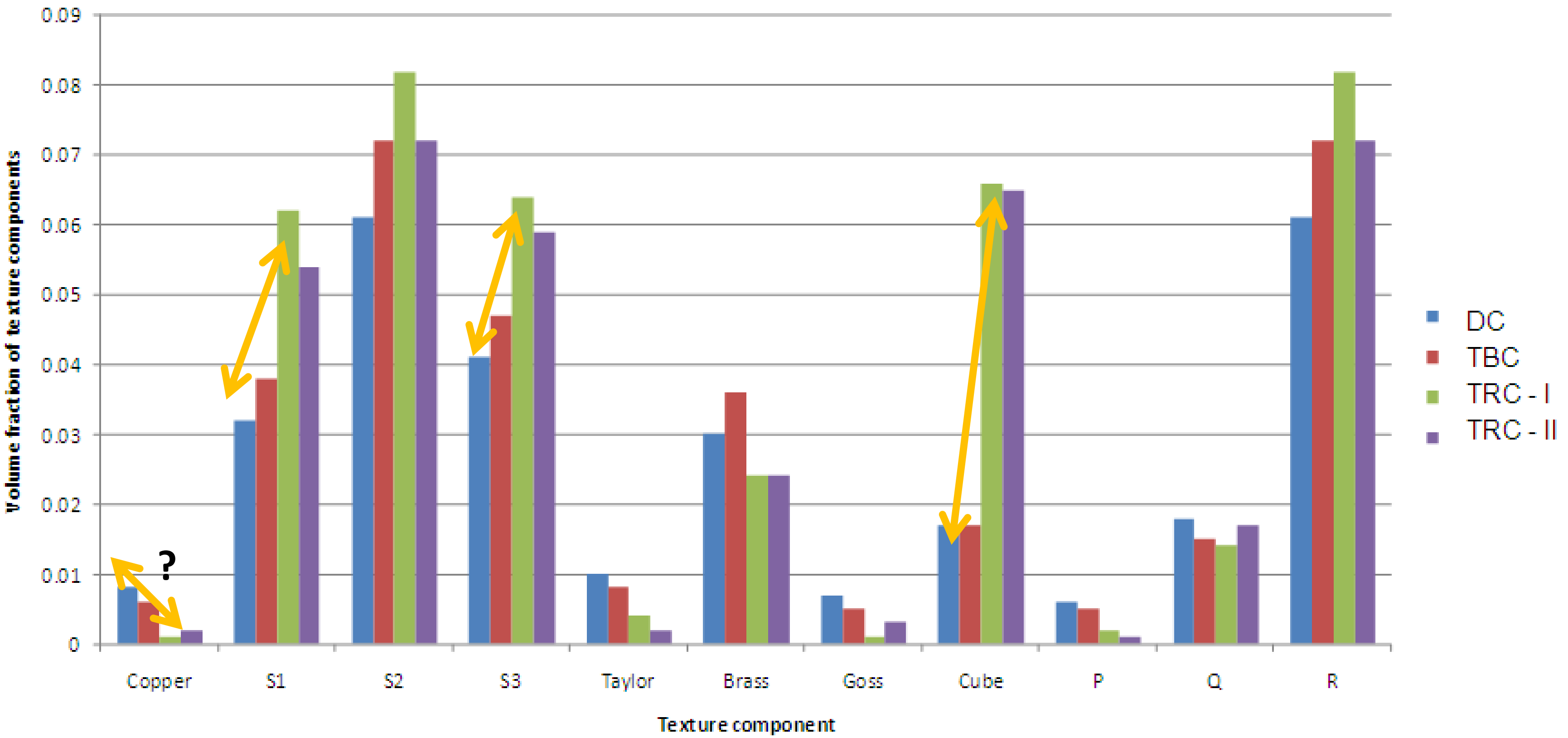

TBC has more rolling texture while TRC has more re-crystalization texture

Summary

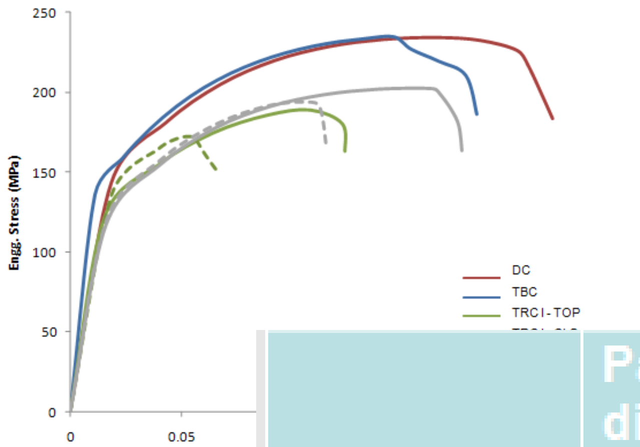

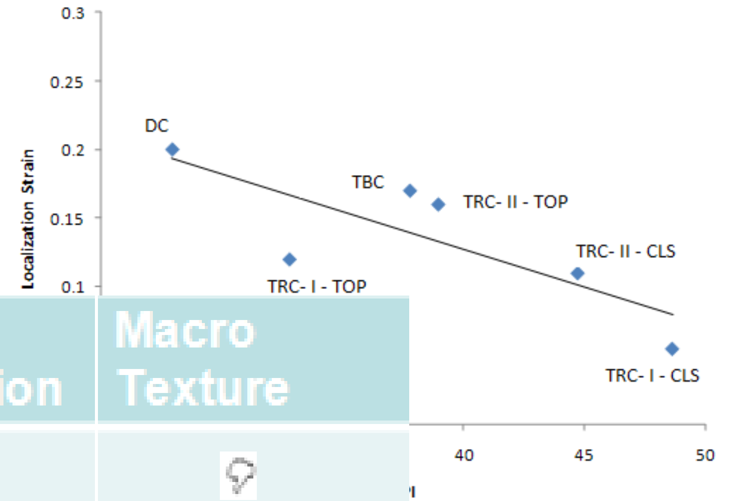

	Particle distribution	Macro Texture
DC	👍	👎
TB CC	👍 👎	👎
TR CC –I	👎	👍
TR CC– II	👍 👎	👍

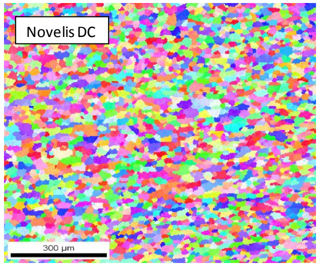

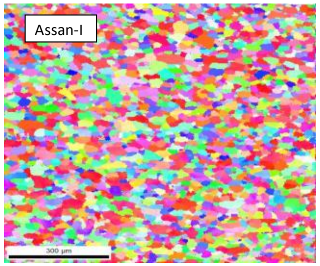

Rolling Direction

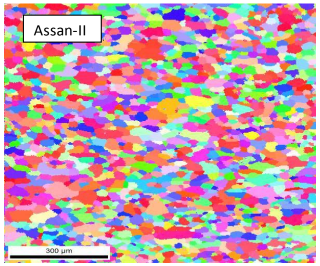

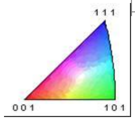

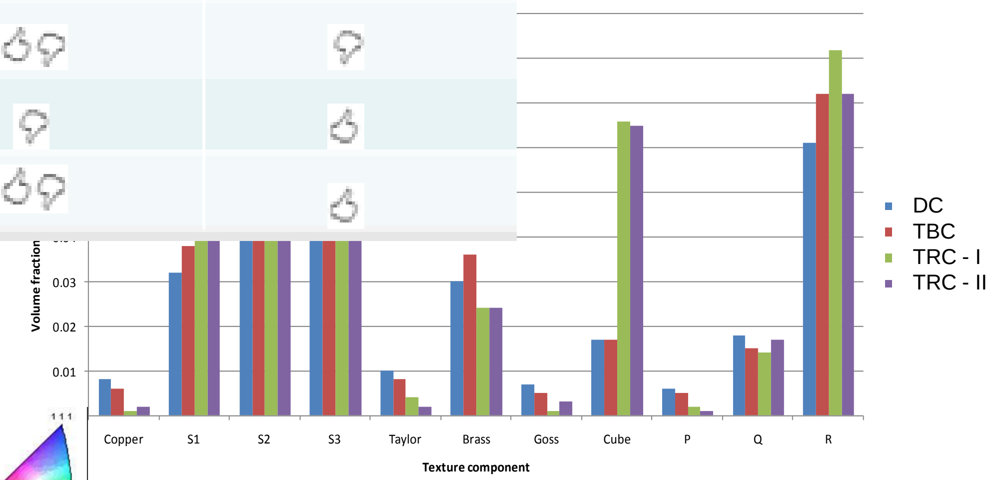

Conclusion

Multi-scale Multimodality Microstructure plays a central role in manufacturing processes.

1.) Machined surface quality and performance is a stronger function of microstructure.

2.) In forming particle distribution and texture can work in cross purpose.